

Rochester Institute of Technology

## RIT Digital Institutional Repository

---

### Theses

---

5-1-2008

## Synthesis and characterization of photoplastic siloxane based thiol-ene polymer systems

Siddhesh Pawar

Follow this and additional works at: <https://repository.rit.edu/theses>

---

### Recommended Citation

Pawar, Siddhesh, "Synthesis and characterization of photoplastic siloxane based thiol-ene polymer systems" (2008). Thesis. Rochester Institute of Technology. Accessed from

This Thesis is brought to you for free and open access by the RIT Libraries. For more information, please contact [repository@rit.edu](mailto:repository@rit.edu).

# **Synthesis and Characterization of Photoplastic Siloxane based Thiol-ene Polymer Systems**

**Siddhesh N. Pawar**

**May 2008**

Thesis submitted in partial fulfillment of the requirements for the degree of Master of Science in  
Chemistry

Approved: \_\_\_\_\_  
Thomas W. Smith (Advisor)

\_\_\_\_\_  
Paul Rosenberg (Department Head)

**Department of Chemistry  
Rochester Institute of Technology  
Rochester, New York 14623-5603**

**Abstract.** Photoplasticity is a phenomenon wherein the shape of crosslinked polymers, under stress, can be induced to change by irradiation with light.<sup>1</sup> Photoplasticity in crosslinked polymer systems *via* stress relaxation has been reported in polyether-acrylate thiol-ene polymer systems by incorporating allyl thioether functionality by ring-opening copolymerization with 6-methyl-3-methylene-1,5-dithiacyclooctane (MDTO). The object of the present work is to adapt the photoplastic stress relaxation approach to demonstrate shape change in silicone elastomers. The apparent way to achieve this is end is to replace the polyether-acrylate thiol-ene monomers, employed in the published literature, with multi-functional silicone-thiols and alkenyl end-functional siloxanes chain extended with MDTO. While homogeneous amorphous elastomeric siloxane-based thiol-enes are well known, it was found that copolymerization of MDTO with the thiol-ene siloxane monomers leads to formation of stable heterogeneous polymer emulsions. Such behavior of thiol-ene siloxanes in the presence of MDTO was found to be a result of the tendency of MDTO to homopolymerize and incipient immiscibility in solutions of MDTO and functionalized siloxane oligomers. The nature of the emulsion formed and extent of crosslinking can depend on factors such as the reactivity of the alkene, the nature of the thiol component and the type of initiation process used. Given that the ring-opening of MDTO was initiated from the multifunctional siloxane thiol, the degree to which chemically different dialkenyl siloxanes were incorporated in the reaction was investigated. Irrespective of the reactivity of the alkene, homopolymerization of MDTO and formation of heterogeneous emulsions and gels always resulted when either the thiol, the ene or both were derived from siloxane oligomers.

## Contents

Introduction.....	1
<i>Actively Moving Polymers</i> .....	1
<i>Photoinduced Plasticity</i> .....	5
<i>Thiol-ene Chemistry</i> .....	12
<i>Thiol-ene Siloxanes</i> .....	17
<i>The Current Research</i> .....	18
Experimental   18	
<i>Materials</i> .....	19
<i>Instrumentation</i> .....	20
<i>Synthesis of Polymers</i> .....	21
Results and Discussion .....	29
<i>Characterization of MDTO</i> .....	29
<i>Demonstration of Photoinduced Plasticity</i> .....	31
<i>Photoplasticity in Siloxanes</i> .....	32
<i>Characterization of Emulsions</i> .....	41
<i>Photoinitiated Polymerizations</i> .....	42
<i>Copolymers with HDT</i> .....	45
<i>Copolymers with PETMP</i> .....	49
Conclusions and Future Directions.....	50
References.....	52

## **List of Figures**

Figure 1: Mechanism in a thermal shape memory polymer with thermal switching temperature $T_{trans}$ .....	2
Figure 2: Molecular mechanism in light induced shape memory polymer .....	3
Figure 3: Reversible cyclodimerization in CA type molecules .....	4
Figure 4: Reaction mechanism of chain-transfer within the polymer backbone.....	6
Figure 5: Monomer structures used to produce the photoplastic networks.....	7
Figure 6: Radical ring-opening mechanism in MDTO .....	8
Figure 7: Strain profiles in PETMP-TEGDVE polymer with varying concentrations of MDTO.....	8
Figure 8: Stress versus time plots for PETMP-TEGDVE polymer containing varying amounts of MDTO .....	9
Figure 9: Actuation behavior induced by stress relaxation mechanism.....	11
Figure 10: Structure of MDTVE.....	11
Figure 11: Thiol-ene radical chain mechanism.....	13
Figure 12: Three basic types of thiols used in thiol-ene polymerizations.....	15
Figure 13: (A) DSC exotherm of a pure acrylate polymerization process. (B) DSC exotherm of a thiol-ene process .....	16
Figure 14: Oxygen scavenging mechanism in thiol-enes .....	17
Figure 15: Reaction schemes for various thiol-ene copolymerizations with and without MDTO.....	19
Figure 16: $^1\text{H}$ -NMR for MDTO .....	29
Figure 17: UV-Visible spectrum of MDTO in Hexane .....	30
Figure 18: Stress relaxation plot at constant strain of 6%.....	31
Figure 19: (a) stressed samples before irradiation (b) change of shape achieved after irradiation.....	32
Figure 20: $^1\text{H}$ -NMR of MDTO homopolymer (ref. 66) .....	34
Figure 21: $^1\text{H}$ -NMR for THIOL.SIL-VINYLSIL-MDTO copolymer .....	35
Figure 22: $^1\text{H}$ -NMR of THIOL.SIL-NORB.SIL-MDTO copolymer.....	36
Figure 23: $^1\text{H}$ -NMR of THIOL.SIL-METHAC.SIL-MDTO copolymer .....	36
Figure 24: $^1\text{H}$ -NMR spectrum for THIOL.SIL-TEGDVE-MDTO copolymer.....	37
Figure 25: Predicted particle structure for emulsions formed with THIOL.SIL.....	38

Figure 26: Free radical events occurring in a thiol-ene-MDTO copolymer system .....	40
Figure 27: TEM images of THIOL.SIL-NORB-SIL-MDTO copolymer emulsion.....	42
Figure 28: Photoinitiated copolymers of THIOL.SIL-MDTO with (A) VINYL.SIL. (B) NORB.SIL and (C) METHAC.SIL (D) TEGDVE .....	44
Figure 29: $^1\text{H}$ -NMR for HDT-TEGDVE-MDTO copolymer .....	46
Figure 30: $^1\text{H}$ -NMR for HDT-VINYL.SIL-MDTO copolymer.....	47
Figure 31: $^1\text{H}$ -NMR for HDT-NORB.SIL-MDTO copolymer .....	47
Figure 32: $^1\text{H}$ -NMR for HDT-METHAC.SIL-MDTO copolymer .....	48
Figure 33: Proposed hydrosilylation of vinyl ether in MDTVE .....	52

### **List of Tables**

Table 1: Tensile moduli of samples before and after irradiations.....	10
Table 2: T <sub>g</sub> values for PETMP-TEGDVE-MDTO copolymers.....	23
Table 3: DLS data for emulsions obtained using THIOL.SIL .....	41

## **List of Abbreviations**

1. MDTO: 6-methyl-3-methylene-1,5-dithiacyclooctane
2. SMP: shape memory polymers
3. CA: cinnamic acid
4. LCE: liquid crystal elastomers
5. LC: liquid crystals
6. TEGDVE: triethyleneglycol divinylether
7. PETMP: pentaerythritol tetra (3-mercaptopropionate)
8. HDT: 1,6-hexanedithiol
9. MDTVE: 2-methylene-propane-1,3-di(thioethyl vinyl ether)
10. AIBN: 2,2'-azobisisobutyronitrile
11. THF: tetrahydrofuran
12. DMPA: 2,2-dimethoxy-2-phenylacetophenone
13. PTA: phosphotungstic acid hydrate
14. MEHQ: 4-methoxyphenol
15. THIOL.SIL: (4-6% mercaptopropylmethylsiloxane)-dimethylsiloxane copolymer
16. VINYL.SIL: vinyl terminated polydimethylsiloxane
17. NORB-SIL: (bicycloheptenyl)ethyl terminated polydimethylsiloxane
18. METHAC.SIL: methacrylate terminated polydimethyl siloxane
19. NMR: nuclear magnetic resonance
20. DSC: differential scanning calorimetry
21. DLS: dynamic light scattering
22. TEM: transmission electron microscope



## Acknowledgements

There is large number of people who have been a source of inspiration and support for me over the two year period of my graduate thesis that I would like to thank deeply. Most important of all I would like to thank my graduate advisor Dr. T. W. Smith for being an excellent mentor and for all the guidance and support he has provided me. I feel extremely privileged to have worked with Dr. Smith and to have learned from him about the ways to perform effective chemistry. His teachings in the classroom and the laboratory have provided me with a strong platform to carry out my future endeavors.

I would like to thank the faculty members in the Department of Chemistry at RIT who have taught me in the classroom and equipped me with all the necessary knowledge and skills. A special thanks to Dr. Gerald Tackas and Dr. Massoud Miri for serving on my graduate committee and being a constant guiding source.

I would like to offer my thanks to Bausch & Lomb for offering financial support to carry out this project. A special thanks to Dr. J. Kunzler for taking out time from his busy schedule to serve on my graduate committee. I also offer my sincere thanks to the other personnel at B&L namely – Dr. Dharmendra Jani, Dr. Ivan Nunez and Dr. Jeff Linhardt for their inspiration and support.

I offer my heartfelt thanks to Mr. Richard Hailstone and Mr. Gary DiFrancesco for their co-operation with TEM and DLS measurements. I also thank Dr. Chang-Feng Ge for providing access to the Instron universal testing machine.

My sincere thanks to Mr. Tom Allston for the help he has provided with the instrumentation involved in this thesis. I thank all the stockroom personnel for providing the chemicals and necessary laboratory equipments as and when I needed them. I also offer my heartfelt thanks to Mrs. Brenda Mastrangelo for all the administrative help provided by her over the past two years.

I would like to congratulate Mr. Glen Labenski and Ms. Jingjing Pan for the excellent work they have carried out as a part of the TWS research group and thank them for their help as co-workers. I also congratulate and thank the entire chemistry graduate cohort at RIT.

I would like to offer my thanks to the current and past faculty in the Paint and Polymer department at U.I.C.T, Mumbai for the teachings they have given me as an undergraduate student. I offer my special and sincere thanks to Prof. V. C. Malshe for being an influential figure in my life, both as a researcher and a mentor.

Finally I offer my thanks to all friends and family back home, especially Mom and Dad for their constant love and support. A special thanks to Snehal for standing proudly besides me through times thick and thin. Without your unconditional love and affection this would not have been possible.

## Introduction

Stimuli responsive polymers are materials that can undergo changes in one or more of their macroscopic properties in response to any of a variety of forces or energy sources. Polymers that respond to stimuli by moving actively and changing their shape have been termed as “actively moving polymers”.<sup>2</sup> Photoplasticity is an active moving behavior in which actuation is achieved using light as stimulus<sup>1</sup> for stress relaxation in crosslinked networks. This relatively new phenomenon has, thus far, been demonstrated in carbon chain polymer systems. A unique objective of the present research is to synthesize silicone-based polymer gels in which photoplasticity can be observed.

### *Actively Moving Polymers*<sup>2</sup>

‘Shape memory polymers’ are a classic actively moving polymer system in which a semicrystalline thermoplastic or thermoset elastomer is deformed and fixed to a new shape. The material can be converted back to its original thermodynamically stable shape by application of a triggering stimulus. A second category of actively moving polymers is ‘shape changing polymers’; these are polymers that are in “an actuated state” as long as a stimulus is applied. When the stimulus is turned off the object returns back to its original state. Liquid crystalline polymers are one instantiation of this category.

Shape memory polymers [SMP] have been an area of extensive research for more than two decades.<sup>3-5</sup> SMP’s are networks containing tie points and suitable switching elements, that are sensitive to the external stimulus applied. A set of network points define the initial state of the material and its permanent shape. These network points may exist in the form of chemical (covalent bonds) or physical (intermolecular interactions) links. Application of the required

stimulus activates the molecular switches and allows for the formation of a new temporal shape. The switches can be re-activated by a trigger of the same or a different stimulus. **Figure 1** depicts the process in a thermal shape memory polymer having permanent crosslinked points and thermally labile tie points.<sup>6</sup> The permanent network points define the thermodynamically stable state and the thermally labile segments ( $T_{trans}$ ) act as switching elements.

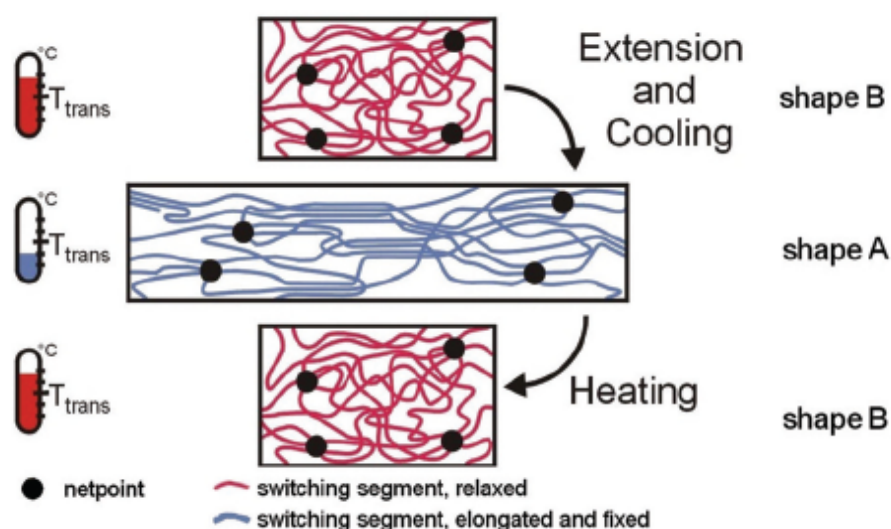


**Figure 1:** Mechanism in a thermal shape memory polymer with thermal switching temperature  $T_{trans}$

Light energy has also been used as a trigger to induce shape memory effects in polymers.<sup>7-9</sup> **Figure 2** depicts a crosslinked amorphous polymer network in which the covalent links define the permanent shape of the polymer.<sup>9</sup>

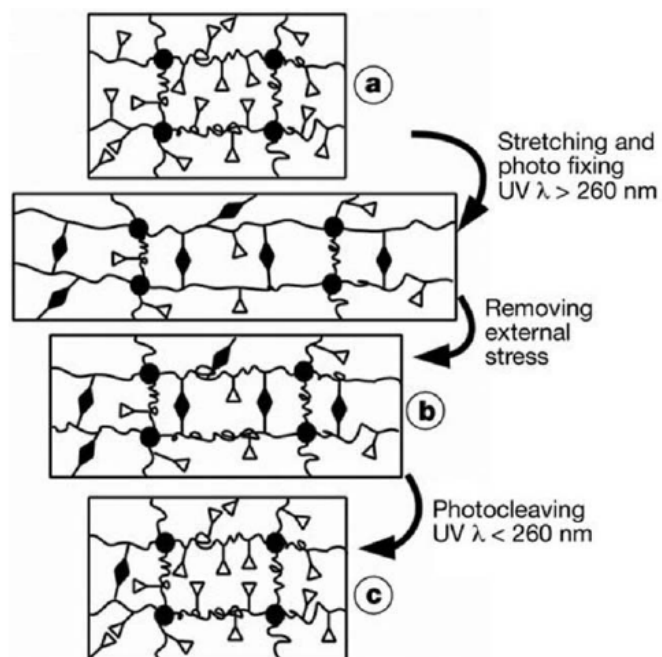


**Figure 2:** Molecular mechanism in light induced shape memory polymer

In state (a) the network is crosslinked at the permanent network points defining the original shape of the polymer. Stretching and photofixing forms covalent bonds that defined a new shape (b) upon removal of stress. Irradiation of the object in state (b) convert the object to state (c), a state which approximates state (a).

Cinnamic acid (CA) ester groups are present and act as reversible photo switches. The CA-ester functional groups cyclodimerize (2 + 2 cycloaddition) with each other upon irradiation with a suitable wavelength fixing the polymer to a new temporary shape. Irradiation with a different wavelength breaks the bonds and the original shape is realized again. **Figure 3**, below shows the scheme for the reversible reaction.<sup>9</sup>

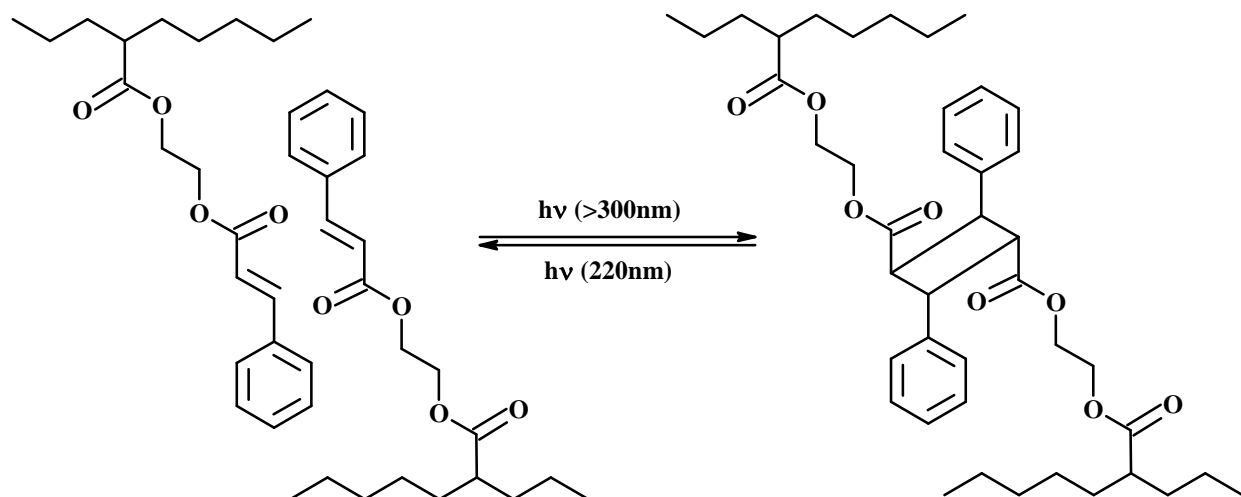


**Figure 3:** Reversible cyclodimerization in CA type molecules

Other than direct actuation by applying heat or light, indirect actuation of thermal shape memory effect has been realized through application of infrared light<sup>10, 11</sup>, electric field<sup>12</sup> and magnetic field.<sup>13</sup>

Shape changing polymers operate on a principle that is different from shape memory polymers. While the permanent shape remains constant in shape changing polymers, the geometry of the temporary shape attained cannot be varied cyclically. This is unlike SMP where the temporary shape required can be programmed to a desired configuration. Thermal shape changing effects in polymers are often based on phase transitions occurring in semicrystalline and liquid crystalline elastomers (LCE).<sup>14-24</sup> It was first predicted by DeGennes<sup>25</sup> that phase transitions in liquid crystals (LC) could lead to mechanical stress or strain. In pure LCs, this strain presents itself in the form of flow anisotropy. Tethering the oriented LC moieties to a crosslinked elastomeric polymer prevents flow and manifests the phase transitions in the form of polymer actuation behavior.

Light-induced shape change behavior has been demonstrated by using photoactive functional groups as molecular switches. Prominent among such groups are azobenzenes and

triphenylmethane leuco derivatives.<sup>26-30</sup> Incorporation of triphenylmethane leuco dyes and subsequent irradiation leads to photo-generation of charged dye molecules. Electrostatic repulsion between such photo-generated charged species causes the polymer to expand or contract resulting in actuation behavior. Upon irradiation with UV light, azobenzene moieties undergo *cis-trans* isomerization resulting in changes in molecular lengths and dipole moment. This transition is reversible from *trans-cis* upon irradiation with light of a different wavelength. Linking the azobenzene groups in an elastomeric polymer causes actuation on exposure to UV light.

Thus ‘shape memory’ behavior and ‘shape changing’ behavior are the two well known categories of actively moving polymers. Photoinduced plasticity is a novel concept which bears some points of distinctions from the traditionally known actively moving polymers.

### ***Photoinduced Plasticity***

In crosslinked elastomers, the equilibrium shape is defined by the shape at gelation. Photoinduced plasticity is a phenomenon wherein the shape of a crosslinked elastomer can be changed plastically by mechanism of stress relaxation. Stress relief enables a sample to be de-stressed from a deformed (stressed) state, thus, creating new equilibrium post-stress-relief shape.

The first published report on photoinduced plasticity in crosslinked polymers describes a covalently crosslinked polymer network capable of undergoing photo-mediated reversible cleavage of its backbone, thereby enabling stress relaxation.<sup>1</sup> The basis of this reversible cleavage is a chemical reaction called the addition-fragmentation chain transfer reaction. This addition-fragmentation chain transfer process occurs in networks of polymers containing allyl thio-ether groups that can be activated by a free-radical initiator. Allyl thioether groups are known to be very good as chain transfer agents.<sup>31-33</sup> In a crosslinked polymer network, a

diffusing radical adds to the carbon-carbon double bond of the allyl thioether group, generating an intermediate that fragments creating a thiol radical and a new allyl thioether group. The process is thus a self-regenerative process which continues as long as free radicals are generated from initiator molecules. **Figure 4**, below, shows the mechanism of the addition-fragmentation chain transfer process occurring within the polymer backbone.<sup>1</sup>

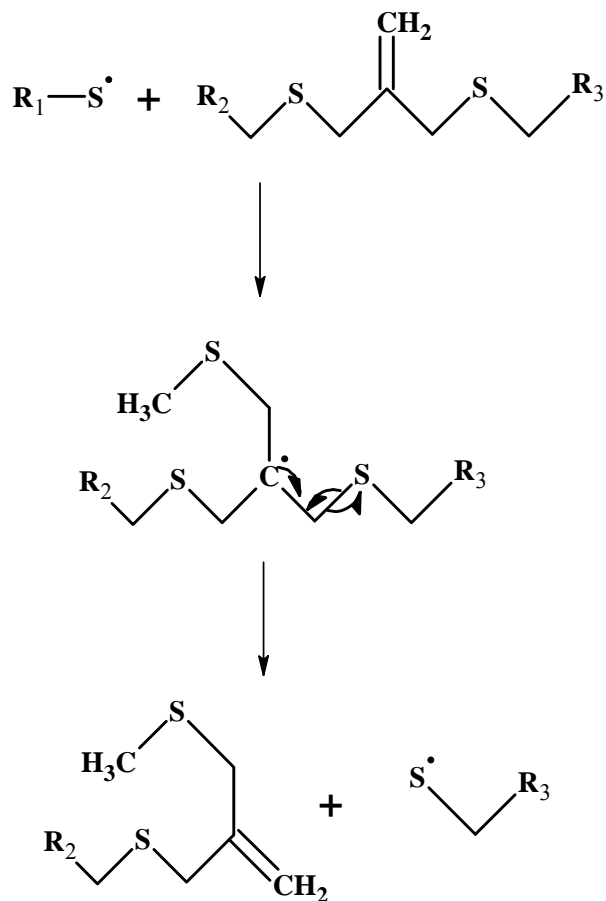


**Figure 4:** Reaction mechanism of chain-transfer within the polymer backbone

The number of addition events is accompanied by equal number fragmentation events; accordingly, the occurrence of addition-fragmentation chain events is characterized by the fact that the effective bond order in the polymer matrix remains unchanged.

The base network employed in the work published by Bowman et.al.<sup>1</sup> is a crosslinked thiol-ene polymer in which the monomeric components were triethyleneglycol divinylether





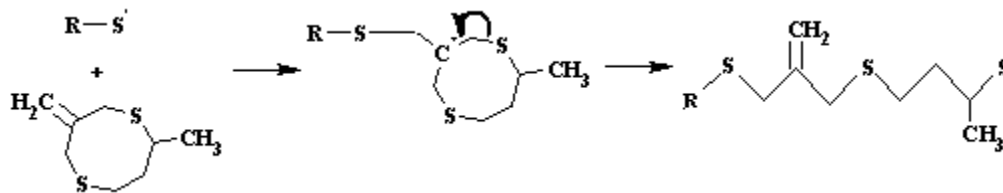


**Figure 6:** Radical ring-opening mechanism in MDTO

Stress relaxation at allyl thioether groups in thiol-ene polymers was demonstrated by Bowman et.al. by generating stress/strain plots.<sup>1</sup> **Figure 7** shows published strain profiles of a PETMP-TEGDVE polymer containing varying concentrations of MDTO. The solid line represents 0 wt% MDTO; the dashed line represents 25 wt% MDTO; dotted line represents 50 wt% MDTO; the dashed-dotted line represents 75 wt% MDTO. The specimens were held under a constant tensile stress throughout the experiment and the corresponding changes in strain were measured. Irradiation was carried out in the presence of a free-radical photo-initiator to induce stress relief.

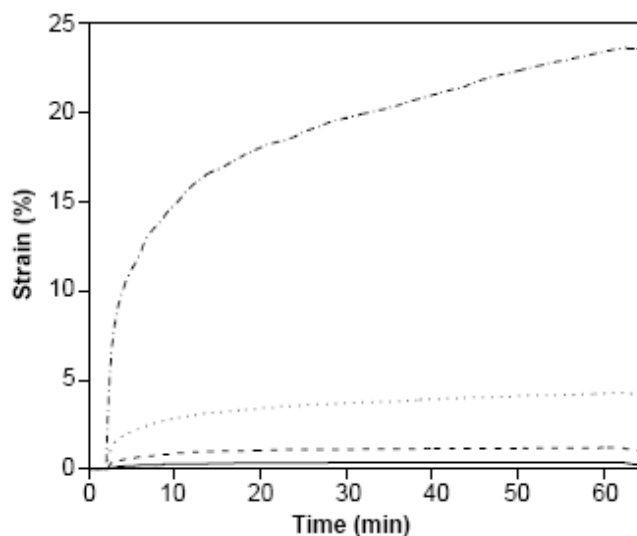


**Figure 7:** Strain profiles in PETMP-TEGDVE polymer with varying concentrations of MDTO

Irradiation of the stressed samples, doped with *bis*-(2,4,6-trimethylbenzoyl)-phenylphosphineoxide [Irgacure 819], results in generation of free radicals which diffuse through the elastomer affecting addition-fragmentation chain transfer among the randomly distributed

allyl thioether groups. Scission of the crosslinked network and reformation of links in an alternate low-stress state induces relaxation of the stress and change of shape of the elastomer, measured in terms of the change in % strain. As seen in the **Figure 7**<sup>1</sup>, a neat PETMP-TEGDVE sample exhibits only a small increase in the strain, which is primarily a thermal effect caused by exposure to UV light. An increase in the MDTO concentration results in an increased density of allyl thioether groups in the network. Thus, the rate of bond breaking and reformation is greater at higher MDTO concentrations, yielding a substantive increase in the % strain.

Bowman et.al. also performed stress relaxation experiments wherein the samples were deformed and held constant at a known value of strain, followed by irradiation to relieve the stress which is measured as a function of time. **Figure 8A** shows a stress relaxation plot where the all samples are stretched to a constant initial strain before irradiation. **Figure 8B** depicts a stress relaxation plot where all samples are stretched to a constant initial stress before irradiation.<sup>1</sup> The solid line represents 0 wt% MDTO; the dashed line represents 25 wt% MDTO; the dotted line represents 50 wt% MDTO; and the dashed-dotted line represents 75 wt% MDTO.

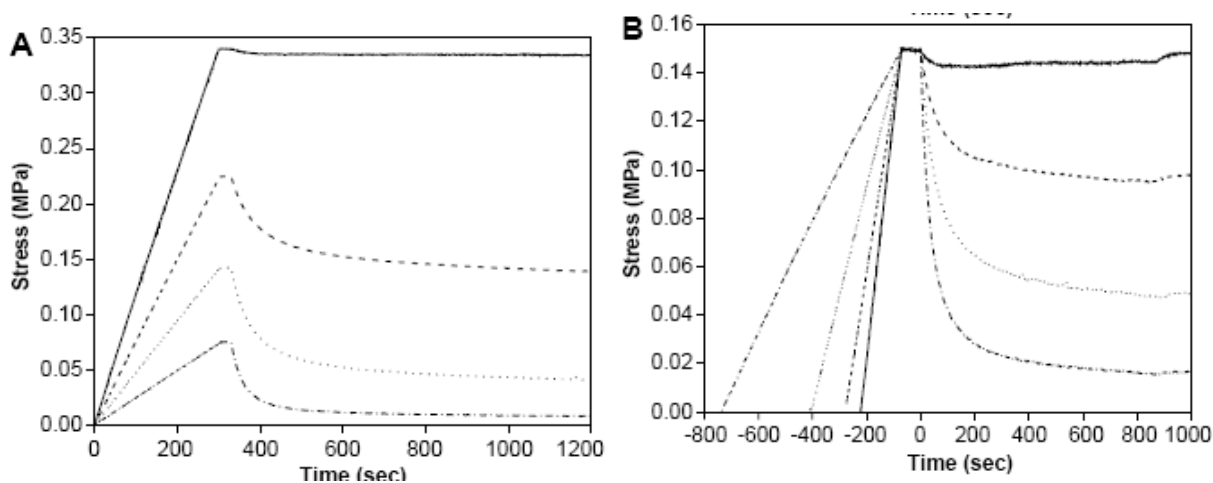


**Figure 8:** Stress versus time plots for PETMP-TEGDVE polymer containing varying amounts of MDTO

An increase in the concentration of MDTO in the polymer, thus, results in an increasing degree of stress-relaxation in the sample. The fact that this effect is not a result of

photodegradation was proven by measuring the elastic modulus of the samples before and after irradiation. **Table 1** shows the recorded tensile modulus values of samples plotted in figure 7A.<sup>1</sup> A slight increase in the modulus, post irradiation, indicates that the effect is not a result of photodegradation.

MDTO (wt%)	Ratio of cross-links to allyl sulfide groups	Modulus before extension and irradiation (MPa)	Modulus after extension and irradiation (MPa)
0	1: 0	11.5	11.8
25	1.17: 1	7.33	7.72
50	0.390: 1	4.58	5.17
75	0.130: 1	2.38	2.92
0 (75 wt % dithiol/divinyl ether)	1: 0	3.21	3.38

**Table 1:** Tensile moduli of samples before and after irradiations

Irradiation of an optically dense polymer film under stress causes relief of stress, on the side at which irradiation is carried out. The stress gradient created causes the film to change its shape to a new equilibrium conformation. Subsequent irradiation from the opposite side causes the unbalanced stresses to be relieved and actuates the film back to a shape approximating the original shape.<sup>1, 38</sup> **Figure 9** depicts the actuation behavior induced by stress relaxation mechanism.<sup>38</sup>

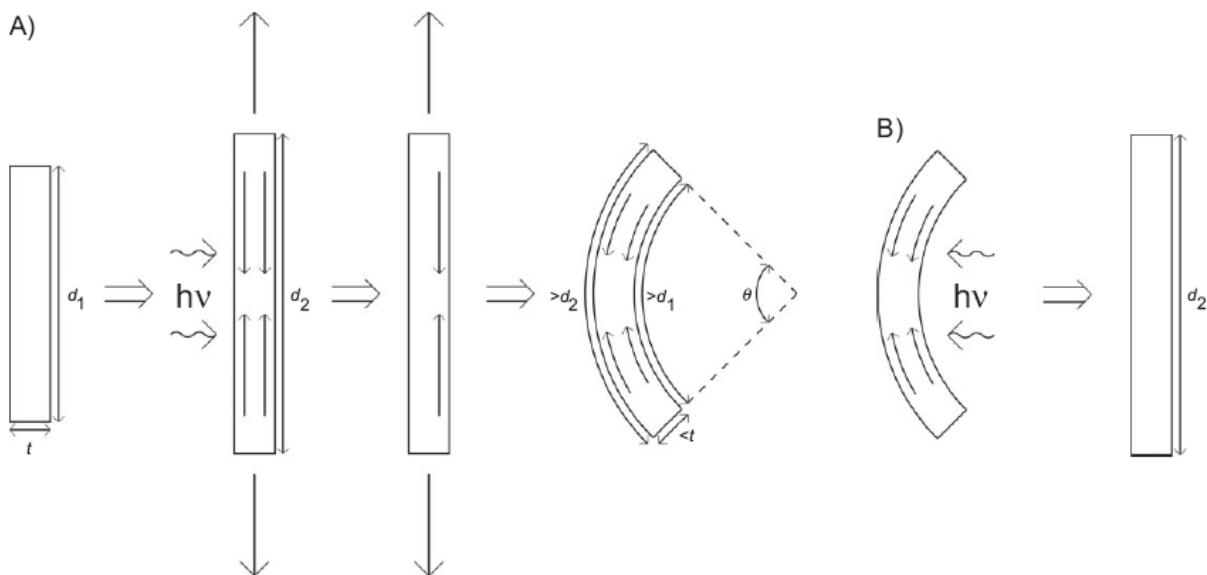


**Figure 9:** Actuation behavior induced by stress relaxation mechanism

Incorporation of allyl thioether groups in a crosslinked thiol-ene polymer backbone has also been reported by using an end functional di-alkene bearing an allyl thioether group.<sup>38</sup> 2-methylene-propane-1,3-di(thioethyl vinyl ether) [MDTVE] was reacted with a multifunctional thiol to create a thiol-ene network bearing allyl thioether groups. **Figure 10** shows the structure of MDTVE.<sup>38</sup>

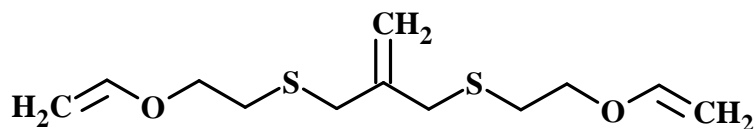


**Figure 10:** Structure of MDTVE

Crosslinked polymers capable of affecting photoplasticity can be used to pattern desirable shapes by creating arbitrary actuation patterns. Masking and selective photolysis of certain regions of the sample has been reported to create objects of distinct geometries.<sup>38</sup> A unique feature of photoplasticity *via* stress relaxation, compared to other photolytic techniques of polymer actuation, is the number of groups activated per photon of light absorbed. Since stress relaxation is a free-radical chain process at the molecular level, each photon absorbed leads to

multiple addition-fragmentation events. In all the other photolytic actuation techniques a single absorbed photon leads to a single event in the process leading to actuation behavior. Photoinduced plasticity, thus, may be advantaged over the other processes known in the literature.

### ***Thiol-ene Chemistry***

The earliest reports on thiol-enes date back to the 1930s and 1950s.<sup>39-41</sup> The first definitive work on photo-initiated polymerization of thiol-ene monomers was published in the 1970s at W. R. Grace. These publications led to a revival of the use of thiol-ene chemistry.<sup>42-46</sup> Since then, extensive and comprehensive reviews were published on this topic by Patai<sup>47</sup> in 1974, Jacobine<sup>48</sup> in 1993 and the Hoyle<sup>34</sup> in 2004.

As shown in **Figure 11**, thiol-enes polymerize by a free radical sequence involving two steps.<sup>48</sup> Step 1 consists in the addition of a thiyl radical to the alkene double bond, creating a carbon centered radical. The radical in step 2 abstracts a hydrogen atom from a thiol group, generating another free thiyl radical thus perpetuating the chain process. Termination occurs via radical-radical coupling.

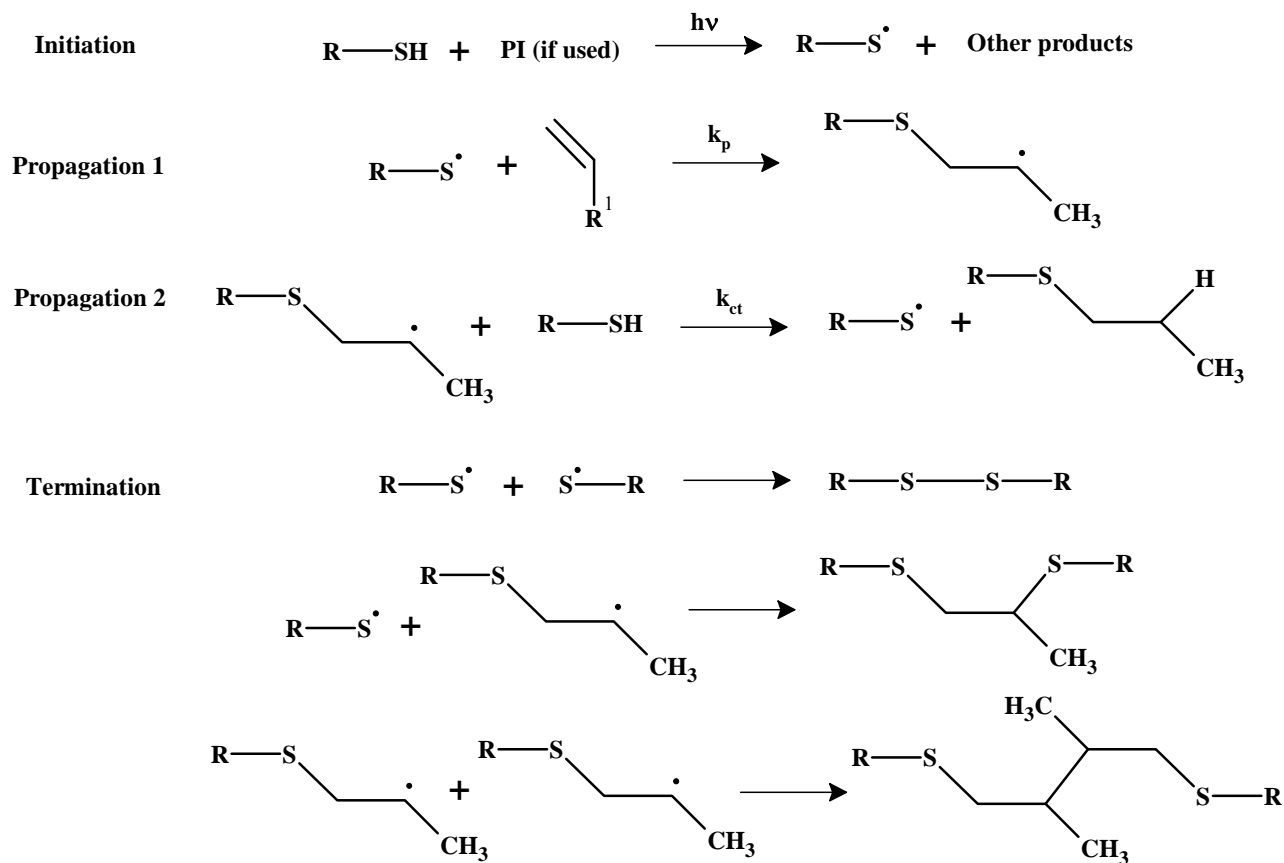


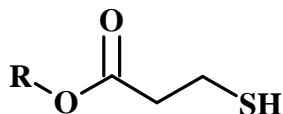
**Figure 11:** Thiol-ene radical chain mechanism

The rate of the thiol-ene reaction depends strongly on the structure of the alkene component used. The general trend relative to the alkene reactivity follows the principle that reactivity is higher for alkenes having higher electron density.<sup>34</sup> A few exceptions to this general thumb rule do exist; for example, in reactivity of norbornenes is higher than expected owing added instability from the ring strain. Similarly, the reactivity of methacrylate, styrene and conjugated dienes is diminished due to resonance stabilization and lower hydrogen abstraction coefficients of their corresponding radicals.

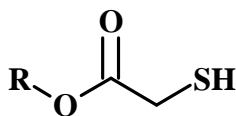
Cramer et al. carried out systematic studies to determine the rate-determining step in the thiol-ene radical mechanism.<sup>49</sup> Their results indicated that for more reactive double bonds in norbornene and divinylether, neither the propagation step nor the chain transfer step is rate

determining. For less reactive double bonds in acrylate, allyl ether and alkenes, the chain transfer hydrogen abstraction step is the rate determining step. The extent of substitution on the ene is also an important parameter in understanding the thiol-ene reaction.<sup>50-52</sup> As a general rule, highly substituted enes are less reactive than singly substituted enes. It has been reported that for a 1:1 thiol-ene mixture, 1-hexene is 8 times more reactive than *trans*-2-hexene and 18 times more reactive than *trans*-3-hexene. This is an indicator of the fact that steric hindrance plays a crucial role in the two step propagation sequence. Johansson et al.<sup>53, 54</sup> have reported that due to the reversible equilibrium involved in the propagation step, addition of a thiyl radical to a *cis*-ene causes reversible isomerization to form a *trans*-ene. The *trans*-ene then undergoes efficient addition from the thiyl radical.

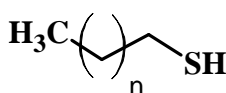
The multifunctional thiols used in thiol-ene polymerizations are typically of one of the following three types – alkyl thiols, thiol glycolate esters and thiol propionate esters. **Figure 12** shows the structures of these thiols.<sup>34</sup> Thiols based on glycolate and propionate esters show higher reactivity due to weakening of the S-H bond by intramolecular hydrogen bonding with the ester carbonyl. The thiols used for crosslinking purposes are generally tri-functional or tetra-functional. Hoyle<sup>34</sup> in his review, provides a complete list of the commonly used commercial thiols. Higher functional thiols have been reported to be synthesized by Woods et al. by the reaction of thiol groups with a dinorbornene compound.<sup>55</sup> Hyperbranched thiols with functionality as high as sixteen have been also reported in the literature.<sup>56-58</sup>



**Alkyl-3-(mercaptopropionate)**



**Alkylthioglycolate**



**Alkyl thiol**

**Figure 12:** Three basic types of thiols used in thiol-ene polymerizations

An interesting feature of thiol-ene polymerizations is their delayed onset of gelation, compared to traditional acrylate systems. Gel point is the point below which there is predominance of low molar mass and linear macromolecular species. At the gel point, a crosslinked network is formed. This network may be swollen with low molar mass and linear macromolecular materials. Jacobine et al. have reported that the gel point in a thiol-ene polymerization process can be engineered by controlling the functionality of the monomers used.<sup>59</sup> It has also been reported that the gelation tendency in a thiol-ene process is much different than traditional acrylate polymerizations. In thiol-enes, gel networks are formed at much higher conversions compared to acrylates. A direct result of this is that there is much less stress build-up in the thiol-ene networks subsequent to network formation.

Unlike vinyl and acrylic free-radical polymerizations, where the presence of small amounts of oxygen strongly inhibits the polymerization process, thiol-ene systems are relatively



insensitive to the presence of oxygen. **Figure 13** shows exotherms generated in an acrylic polymerization process (A) and a thiol-ene process (B) in both nitrogen and air.<sup>34</sup>

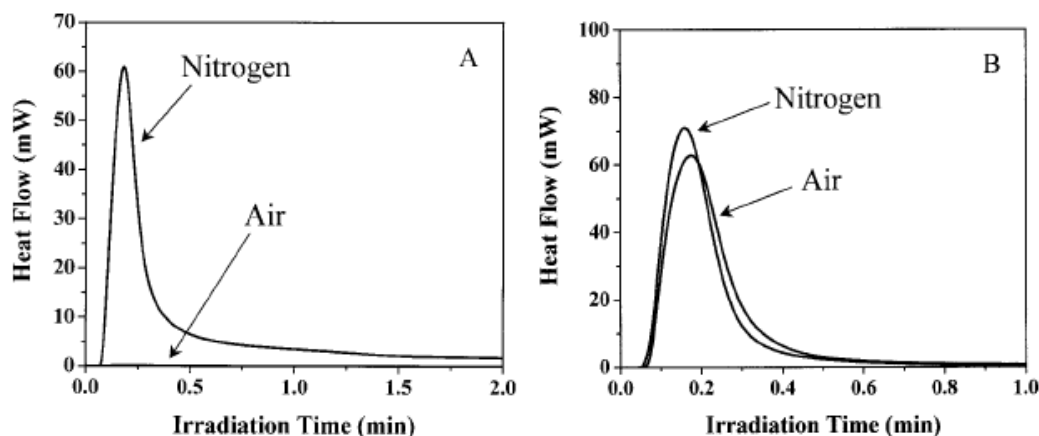


**Figure 13:** (A) DSC exotherm of a pure acrylate polymerization process. (B) DSC exotherm of a thiol-ene process

An explanation to the theory behind a thiol-ene process being relatively insensitive to oxygen inhibition was provided by Gush et al.<sup>60</sup> It is reported that the peroxy radicals formed by the reaction of the carbon centered propagating radicals with molecular oxygen maintain their ability to abstract hydrogens from the thiol groups, thus, avoiding radical termination. **Figure 14** shows a depiction of the molecular process.<sup>34</sup>

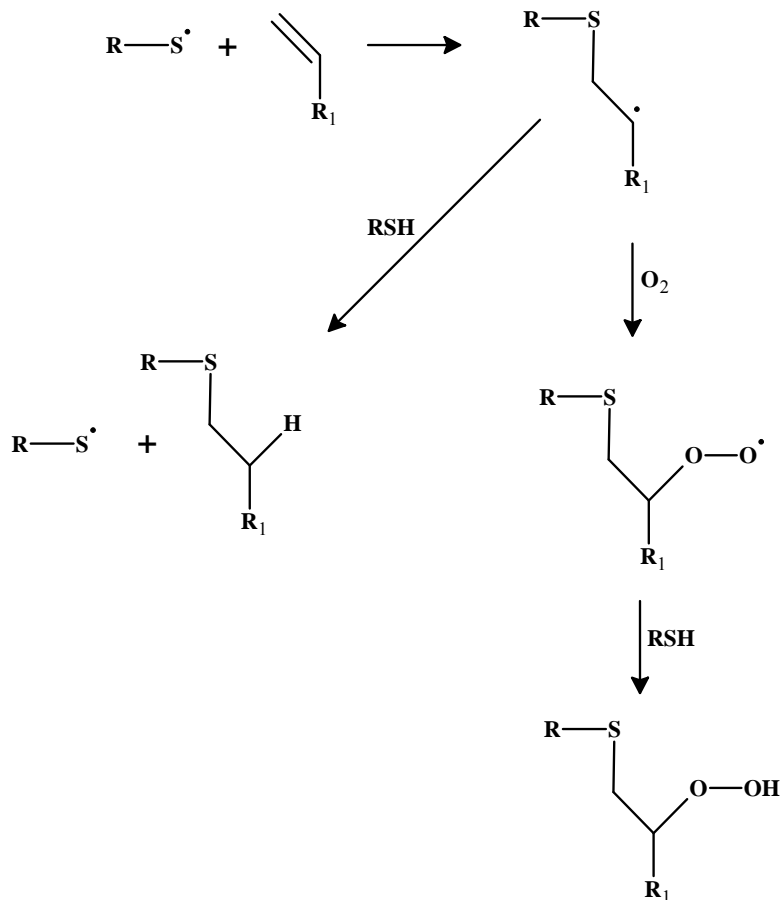


**Figure 14:** Oxygen scavenging mechanism in thiol-enes

### *Thiol-ene Siloxanes*

Due to their unique properties (insensitivity to oxygen and delayed gelation) and potential applications, crosslinked siloxane polymers are a topic of significant interest. The majority of the developmental efforts in the area of photocrosslinkable siloxanes have been focused on the extension of vinyl siloxanes to traditional platinum addition cure systems and acrylic silicones.<sup>61</sup> The photocrosslinking of vinylsiloxane fluids with mercapto functional silicones has been studied for the past 20 years.<sup>62</sup>

In a paper published in 1992, Jacobine<sup>63</sup> reviewed the silicone monomers, oligomers and resins used in photopolymerizable compositions. A review of thiol-ene

photopolymers was published by Jacobine.<sup>48</sup> Müller and Kunze<sup>64</sup> published an article relating specifically to the photoinduced thiol-ene crosslinking of modified silicones. Jacobine et al.<sup>65</sup> have also described the photocrosslinking of norbornene resins with multifunctional thiols.

### ***The Current Research***

Research described in this thesis provides an extension to the work published by Bowman et al.<sup>1, 38</sup> Previously published reports on photoinduced plasticity in crosslinked polymers report on organic polymer systems having carbon-chain backbones embedded in the well-studied thiol-ene chemistry. The point of departure for the current research is the exploration of the phenomenon of photoplasticity in thiol-ene polymers which possess predominantly siloxane backbones.

The initial objective was to synthesize and characterize photoplastic thiol-ene siloxane polymers by mimicking Bowman type systems with functional siloxanes. The organic thiol (PETMP) and ene (TEGDVE) monomers used by Bowman are replaced by a multifunctional siloxane thiol and a difunctional siloxane ene. The active component of the monomer mixture that imparts photoplasticity, MDTO, is kept constant.

Although the copolymerization of MDTO with the thiol-ene monomers was expected to proceed to yield a homogeneous, crosslinked network, irrespective of the nature of the thiol and ene monomer backbones, it was found that with functional siloxane monomers formation of a homogeneous crosslinked polymer network was frustrated. In our initial experiments, control reactions, outlined in the **Figure 15** below, between PETMP and TEGDVE; PETMP, TEGDVE and MDTO; and siloxane thiol and siloxane alkene were carried out to yield, in all cases, clear gels. The PETMP, TEGDVE, MDTO systems was determine to be photoplastic, duplicating

results report by Bowman, et al. When MDTO was incorporated in the siloxane thiol/siloxane alkene system a sterically stabilized emulsion was obtained.

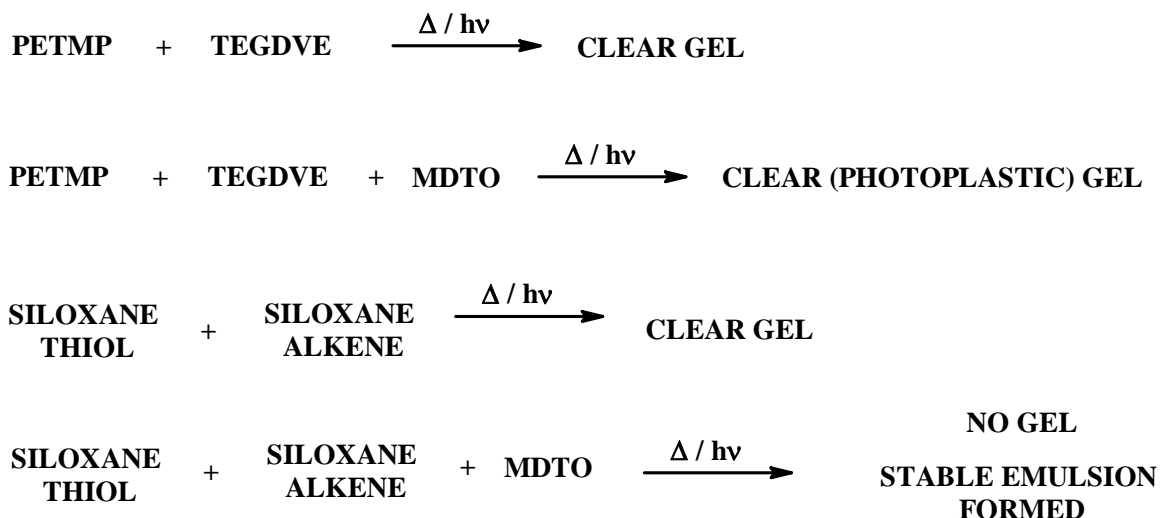


**Figure 15:** Reaction schemes for various thiol-ene copolymerizations with and without MDTO

Based on these findings, the primary objectives of the present research are to:

- ✓ explore the effect of the reactivity of the ene component on the incorporation of MDTO
- ✓ elucidate details of the copolymerization/homopolymerization behavior of MDTO in thiol-ene siloxane systems.
- ✓ compare the copolymerization in thermally initiated systems with that in photoinitiated systems.
- ✓ explore alternative routes to the formation of photoplastic siloxane elastomers

## Experimental

### Materials

3-chloro-2-(chloromethyl)-1-propene (99%) [C31104], sodium borohydride (98%) [452874], sodium metal [483745], pentaerythritol tetrakis(3-mercaptopropionate) [381462] {PETMP}, triethyleneglycol divinylether (98%) [329800] {TEGDVE}, dicumyl peroxide (98%) [329541], 2,2'-azobisisobutyronitrile (98%) [441090] {AIBN} (recrystallized from methanol)

and tetrahydrofuran (99+%) [360589] {THF} were obtained from Sigma-Aldrich. 2,2-dimethoxy-2-phenylacetophenone (99%) [18784] {DMPA}, Phosphotungstic acid hydrate {PTA} and 4-methoxyphenol (99%) [12600] {MEHQ} were obtained from Acros Organics. 1,3-butanedithiol [W352918] and 1,6-hexanedithiol (97%) [W349518] {HDT} were obtained from SAFC. (4-6% mercaptopropylmethylsiloxane)-dimethylsiloxane copolymer (SMS-042) [THIOL.SIL], vinyl terminated polydimethylsiloxane (DMS-V21) [VINYL.SIL] and (bicycloheptenyl)ethyl terminated polydimethylsiloxane (DMS-NB25) [NORB-SIL] were obtained from Gelest Inc. Methacrylate terminated polydimethyl siloxane [METHAC.SIL] was obtained from Silar Laboratories. Methanol and calcium chloride pellets were obtained from J. T. Baker. Toluene [TX0735] was obtained from EMD.

Unless otherwise noted, all reagents were used as received without further purification.

### ***Instrumentation***

Proton NMR spectra were obtained using a Bruker 300MHz. spectrometer. Solvents used were Chloroform-d (99.8% D) or Benzene-d<sub>6</sub> (99.6% D), both obtained from Acros Organics.

Glass transition data was gathered using a TA Instruments DSC 2010 with samples prepared in non-hermetic aluminum pans. All T<sub>g</sub> values are reported as the T<sub>g</sub> midpoint temperatures.

UV Visible spectrometric data was collected on a Hewlett Packard 8453 diode array instrument.

Infrared spectroscopic data was collected on a Shimadzu IR Prestige-21. All data was gathered in absorption mode.

Stress-strain measurements were performed on an Instron 5567 universal mechanical tester operated by Bluehill 2 software.

UV irradiation of samples was performed using UVP model UVGL-25 Mineralight® lamp with a multiband UV light source of 366 nm wavelengths.

Dynamic light scattering [DLS] were carried out by Mr. Gary DiFrancesco (Scientist, Rochester Institute of Technology, Center for Imaging Science) and were performed on a Brookhaven Instruments Corp. 90 Plus particle size analyzer. All measurements were made at an angle of 90°.

Transmission electron microscopy was carried out by Mr. Richard Hailstone (Associate Professor, Rochester Institute of Technology, Center for Imaging Science).

### ***Synthesis of Polymers***

**2-methyl-7-methylene-1,5-dithiaclooctane [MDTO].** MDTO was prepared by adaptation of the procedure reported by Rizzardo et al.<sup>66</sup> Thus, 3-chloro-2-(chloromethyl)-1-propene (12.88 g, 103.04 mMoles) and 1,3-butanedithiol (12.57 g, 103.04 mMoles) were dissolved separately in 60 ml methanol each. The two solutions were added simultaneously *via* two separate feed lines to a refluxing solution of sodium metal (4.97 g, 216.38 mMoles) in 150 ml methanol. The rate of addition was maintained at 5 ml/hr by adding aliquots of 1 ml for every 12 minutes. Post addition, the reaction mixture was refluxed for 5 more hours. A white salt precipitate was formed during the reaction. Methanol was then evaporated after which water was added to dissolve the salt and the solution was extracted with ether. The ether extracts were dried overnight using calcium chloride pellets. Following this the ether was evaporated to give 17.78 g of crude product. The crude was bulb to bulb distilled at 95-100 °C and 0.5 mm pressure to yield 12.98 g clear, pale yellow colored oil. This pale oil was further dissolved in a mixture of

methanol-water-THF and treated with sodium borohydride (0.2843 g, 7.459 mMoles) overnight. Following this the solvents were evaporated, product dissolved in ether and washed with strong aqueous sodium hydroxide. The ether extracts were dried overnight using calcium chloride. Next, ether was evaporated and the oil redistilled bulb-to-bulb at 95-100 °C and 0.5 mm pressure to yield 9.53 g (53.18%) clear, water white product. <sup>1</sup>H-NMR (benzene-d<sub>6</sub>): δ 1.16 (d, 3H), 1.2-1.6 (mult., 2H), 2.5-3.1 (mult., 7H), 4.89 (s, 2H)

**PETMP-TEGDVE-MDTO copolymers.** Stoichiometric mixtures of PETMP and TEGDVE were polymerized in a 1:2 mole ratio. MDTO was incorporated as a co-monomer on weight percent basis with respect to the PETMP-TEGDVE mixtures. Four samples were prepared containing – 0% MDTO, 25% MDTO, 50% MDTO and 75% MDTO. AIBN (1% by weight of the PETMP-TEGDVE-MDTO mixture) was added as a free radical initiator. MEHQ (1% by weight of the PETMP-TEGDVE-MDTO mixture) was added as an inhibitor to prevent the monomers from polymerizing when mixed at room temperature. DMPA (0.1% by weight of the PETMP-TEGDVE-MDTO mixture) was incorporated as a photoinitiator for photo-induced stress relaxation experiments, post-crosslinking. The monomer mixtures were injected between two silanized glass plates spaced by a ~0.5 mm Teflon tape gasket and held together using binder clips. The sandwiched films were then polymerized thermally, heating overnight in a conventional oven at 70 °C. **Table 2** shows the T<sub>g</sub> values of the synthesized polymers.

Sample	T <sub>g</sub> (°C)
0% MDTO	-31.50
25 % MDTO	-33.45
50% MDTO	-35.26
75% MDTO	-36.02

**Table 2:** T<sub>g</sub> values for PETMP-TEGDVE-MDTO copolymers

### ***Demonstration of Photoinduced Plasticity***

**Quantitative demonstration.** PETMP-TEGDVE-MDTO copolymers with varying concentrations of MDTO were used – 0% MDTO, 25% MDTO, 50% MDTO and 75% MDTO. Samples were 1 mm thick and cut into dimensions of 7-9 mm in width and over 20 mm in length. A custom experiment was set up wherein the samples were stretched to a constant strain of 6% by applying a strain rate of 0.4% per min for 15 min. After reaching strain levels of 6% the samples were held constant for 2 min and irradiated thereafter for a period of 15 min. Tensile stresses in the films were measured throughout the experiments as a function of time. Before running each sample, the sample dimensions were fed to the software for accurate stress calculations. Irradiation was performed at a wavelength of 366 nm.

**Qualitative demonstration.** PETMP-TEGDVE-MDTO copolymers with varying concentrations of MDTO were used – 0% MDTO, 25% MDTO, 50% MDTO and 75% MDTO. Samples were 1 mm thick and cut into dimensions of 7 mm in width and 35 mm in length. In order to induce stress the samples were folded into an inverted U-shaped configuration and held between the two jaws of a vice. All the samples were stressed and irradiated simultaneously. Irradiation was carried out such that the samples were exposed for 3 min from the top face and 3



min each from the side faces. Thus the total irradiation time was 9 min. Wavelength of the light source used was 366 nm.

**Thiol-ene siloxane copolymerization of THIOL.SIL-VINYLSIL.** DMPA (1 mg, 3.9  $\mu$ Moles / 0.1% by weight of the monomer mixture) was dissolved in a mixture of THIOL.SIL (0.3556 g, 46.78  $\mu$ Moles), VINYL.SIL (0.6443 g, 107.38  $\mu$ Moles) and MDTO (0.1 g, 574.71  $\mu$ Moles / 25% by weight of THIOL.SIL-VINYLSIL mixture). The mixture was placed on a silanized glass plate within an area bounded by a perimeter of Teflon tape. A quartz window was placed on top to sandwich the monomer mixture and the sample was irradiated using a 366 nm source for 3 minutes. After irradiation a clear crosslinked polymer film was obtained.

**Bulk polymerization of THIOL.SIL-VINYLSIL-MDTO copolymer.** Dicumyl peroxide (5 mg, 18.51  $\mu$ Moles / 1% by weight of the monomer mixture) was dissolved in a mixture of THIOL.SIL (0.01422 g, 18.71  $\mu$ Moles) and VINYL.SIL (0.2577 g, 42.95  $\mu$ Moles). DMPA (1.25 mg, 4.88  $\mu$ Moles / 0.25% by weight of the monomer mixture) was incorporated for possible stress relaxation. The monomer was immiscible at room temperature but turned clear above a temperature of 65-70 °C. The mixtures was then injected between two silanized glass plates spaced by a ~0.5 mm Teflon tape gasket and held together using binder clips. The sandwiched films were then polymerized thermally in a conventional oven at 130 °C overnight. Post-polymerization an emulsion was obtained between the glass plates.

**Thermally initiated THIOL.SIL-VINYLSIL-MDTO copolymer.** AIBN (5 mg, 30.48  $\mu$ Moles / 1% by weight of the monomer mixture) was dissolved in 0.125 ml toluene in a screw cap test-tube. THIOL.SIL (0.1422 g, 18.71  $\mu$ Moles), VINYL.SIL (0.2577 g, 42.95  $\mu$ Moles) and MDTO (0.1 g, 574.71  $\mu$ Moles / 25% by weight of THIOL.SIL-VINYLSIL mixture) was then added to the test tube and mixed thoroughly. The test tube was attached to a water condenser,

maintained under argon pressure and heated in an oil-bath at a temperature of 70 °C for 3 hours. After 3 hours a stable polymer emulsion was obtained having a bluish tinge.

**Thermally initiated THIOL.SIL-NORB.SIL-MDTO copolymer.** AIBN (5 mg, 30.48  $\mu$ Moles / 1% by weight of the monomer mixture) was dissolved in 0.125 ml toluene in a screw cap test-tube. THIOL.SIL (0.0735 g, 9.675  $\mu$ Moles), NORB.SIL (0.3264 g, 23.31  $\mu$ Moles) and MDTO (0.1 g, 574.71  $\mu$ Moles / 25% by weight of THIOL.SIL-NORB.SIL mixture) was then added to the test tube and mixed thoroughly. The test tube was attached to a water condenser, maintained under argon pressure and heated in an oil-bath at a temperature of 70 °C for 3 hours. After 3 hours a stable polymer emulsion was obtained having a bluish tinge.

**Thermally initiated THIOL.SIL-METHAC.SIL-MDTO copolymer.** AIBN (5 mg, 30.48  $\mu$ Moles / 1% by weight of the monomer mixture) was dissolved in 0.125 ml toluene in a screw cap test-tube. THIOL.SIL (0.2530 g, 33.29  $\mu$ Moles), METHAC.SIL (0.1469 g, 80.24  $\mu$ Moles) and MDTO (0.1 g, 574.71  $\mu$ Moles / 25% by weight of THIOL.SIL-METHAC.SIL mixture) was then added to the test tube and mixed thoroughly. The test tube was attached to a water condenser, maintained under argon pressure and heated in an oil-bath at a temperature of 70 °C for 3 hours. After 3 hours a stable polymer emulsion was obtained having a bluish tinge.

**Thermally initiated THIOL.SIL-TEGDVE-MDTO copolymer.** AIBN (5 mg, 30.48  $\mu$ Moles / 1% by weight of the monomer mixture) was dissolved in 0.125 ml toluene in a screw cap test-tube. THIOL.SIL (0.3758 g, 49.45  $\mu$ Moles), TEGDVE (0.0241 g, 119.19  $\mu$ Moles) and MDTO (0.1 g, 574.71  $\mu$ Moles / 25% by weight of THIOL.SIL-TEGDVE mixture) was then added to the test tube and mixed thoroughly. The test tube was attached to a water condenser, maintained under argon pressure and heated in an oil-bath at a temperature of 70 °C for 3 hours. After 3 hours a stable polymer emulsion was obtained having a bluish tinge.

**Thermally initiated HDT-VINYL.SIL-MDTO copolymer.** AIBN (5 mg, 30.48  $\mu$ Moles / 1% by weight of the monomer mixture) was dissolved in 0.125 ml toluene in a screw cap test-tube. HDT (10.25 mg, 68.20  $\mu$ Moles), VINYL.SIL (0.03897 g, 64.95  $\mu$ Moles) and MDTO (0.1 g, 574.71  $\mu$ Moles / 25% by weight of HDT-VINYL.SIL mixture) was then added to the test tube and mixed thoroughly. The test tube was attached to a water condenser, maintained under argon pressure and heated in an oil-bath at a temperature of 70 °C for 3 hours. After 3 hours a milky white stable polymer emulsion was obtained.

**Thermally initiated HDT-NORB.SIL-MDTO copolymer.** AIBN (5 mg, 30.48  $\mu$ Moles / 1% by weight of the monomer mixture) was dissolved in 0.125 ml toluene in a screw cap test-tube. HDT (4.24 mg, 28.26  $\mu$ Moles), NORB.SIL (0.3957 g, 28.26  $\mu$ Moles) and MDTO (0.1 g, 574.71  $\mu$ Moles / 25% by weight of HDT-NORB.SIL mixture) was then added to the test tube and mixed thoroughly. The test tube was attached to a water condenser, maintained under argon pressure and heated in an oil-bath at a temperature of 70 °C for 3 hours. After 3 hours a milky white stable polymer emulsion was obtained.

**Thermally initiated HDT-METHAC.SIL-MDTO copolymer.** AIBN (5 mg, 30.48  $\mu$ Moles / 1% by weight of the monomer mixture) was dissolved in 0.125 ml toluene in a screw cap test-tube. HDT (30.34 mg, 201.88  $\mu$ Moles), METHAC.SIL (369.6 mg, 201.88  $\mu$ Moles) and MDTO (0.1 g, 574.71  $\mu$ Moles / 25% by weight of HDT-METHAC.SIL mixture) was then added to the test tube and mixed thoroughly. The test tube was attached to a water condenser, maintained under argon pressure and heated in an oil-bath at a temperature of 70 °C for 3 hours. After 3 hours a milky white stable polymer emulsion was obtained.

**Thermally initiated HDT-TEGDVE-MDTO copolymer.** AIBN (5 mg, 30.48  $\mu$ Moles / 1% by weight of the monomer mixture) was dissolved in 0.125 ml toluene in a screw cap test-

tube. HDT (170.53 mg, 1.135 mMoles), TEGDVE (229.46 mg, 1.135 mMoles) and MDTO (0.1 g, 574.71  $\mu$ Moles / 25% by weight of HDT-TEGDVE mixture) was then added to the test tube and mixed thoroughly. The test tube was attached to a water condenser, maintained under argon pressure and heated in an oil-bath at a temperature of 70 °C for 3 hours. After 3 hours a clear transparent linear polymer was obtained.

**Photo initiated THIOL.SIL-VINYL.SIL-MDTO copolymer.** DMPA (1.25 mg, 4.88  $\mu$ Moles / 0.25% by weight of the monomer mixture) was dissolved in 0.125 ml toluene. THIOL.SIL (0.1422 g, 18.71  $\mu$ Moles), VINYL.SIL (0.2577 g, 42.95  $\mu$ Moles) and MDTO (0.1 g, 574.71  $\mu$ Moles / 25% by weight of THIOL.SIL-VINYL.SIL mixture) were then added and mixed thoroughly. The monomer mixture was placed on a silanized glass plate, held within Teflon tape boundaries and irradiated at a wavelength of 366 nm for 3 minutes.

**Photo initiated THIOL.SIL-NORB.SIL-MDTO copolymer.** DMPA (1.25 mg, 4.88  $\mu$ Moles / 0.25% by weight of the monomer mixture) was dissolved in 0.125 ml toluene in a screw cap test-tube. THIOL.SIL (0.0735 g, 9.675  $\mu$ Moles), NORB.SIL (0.3264 g, 23.31  $\mu$ Moles) and MDTO (0.1 g, 574.71  $\mu$ Moles / 25% by weight of THIOL.SIL-NORB.SIL mixture) were then added and mixed thoroughly. The monomer mixture was placed on a silanized glass plate, held within Teflon tape boundaries and irradiated at a wavelength of 366 nm for 3 minutes.

**Photo initiated THIOL.SIL-METHAC.SIL-MDTO copolymer.** DMPA (1.25 mg, 4.88  $\mu$ Moles / 0.25% by weight of the monomer mixture) was dissolved in 0.125 ml toluene in a screw cap test-tube. THIOL.SIL (0.2530 g, 33.29  $\mu$ Moles), METHAC.SIL (0.1469 g, 80.24  $\mu$ Moles) and MDTO (0.1 g, 574.71  $\mu$ Moles / 25% by weight of THIOL.SIL-METHAC.SIL mixture) were then added and mixed thoroughly. The monomer mixture was placed on a

silanized glass plate, held within Teflon tape boundaries and irradiated at a wavelength of 366 nm for 3 minutes.

**Photo initiated THIOL.SIL-TEGDVE-MDTO copolymer** DMPA (1.25 mg, 4.88  $\mu$ Moles / 0.25% by weight of the monomer mixture) was dissolved in 0.125 ml toluene in a screw cap test-tube. THIOL.SIL (0.3758 g, 49.45  $\mu$ Moles), TEGDVE (0.0241 g, 119.19  $\mu$ Moles) and MDTO (0.1 g, 574.71  $\mu$ Moles / 25% by weight of THIOL.SIL-TEGDVE mixture) were then added and mixed thoroughly. The monomer mixture was placed on a silanized glass plate, held within Teflon tape boundaries and irradiated at a wavelength of 366 nm for 3 minutes.

**Sample preparation for TEM.** 3-4 drops of the emulsion were placed in a test-tube and 3 ml methanol was added. Methanol does not dissolve the emulsion particles and an oily layer is formed at the bottom of the test tube. THF is then added until the layer dissolves and a homogenous but hazy solution is obtained. A copper coated carbon grid is dipped multiple number of times in this solution and dried in air. The grid is then imaged under the TEM.

**Sample preparation for DLS.** Samples prepared by in the TEM sample preparation were used to obtain DLS data by further dilution with THF.

## Results and Discussion

### *Characterization of MDTO*

MDTO was synthesized by a procedure analogous to that published by Rizzardo et al.<sup>66</sup> and outlined in the experimental section. Characterization was performed by  $^1\text{H}$ -NMR using benzene- $\text{d}_6$  as solvent. **Figure 16** shows the NMR spectrum obtained for the synthesized molecule.

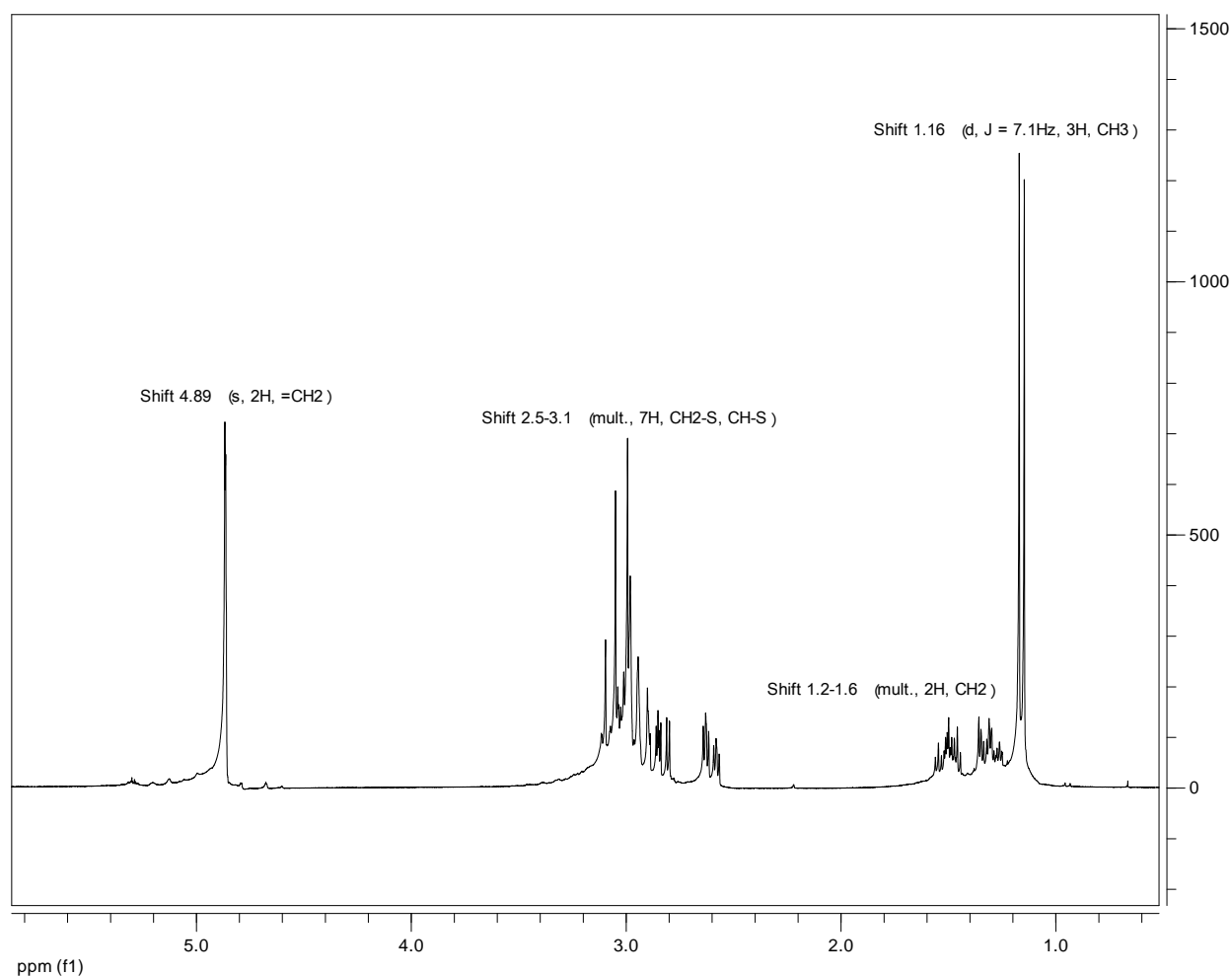


**Figure 16:**  $^1\text{H}$ -NMR for MDTO

MDTO is a clear colorless liquid at room temperature, but solidifies at on reffridgeration. On reheating it turns into liquid and remains in that state until and unless cooled again. **Figure**

**17** shows the UV-Visible spectrum obtained for MDTO in Hexane as solvent. The spectrum shows that the UV absorption maximum appears at 234 nm and there is no absorption above 367 nm. Thus in order to irradiate films containing MDTO across the entire thickness, light of wavelength greater than 366-367 nm will have to be used. Therefore in our experiments we use a light of wavelength 366 nm.

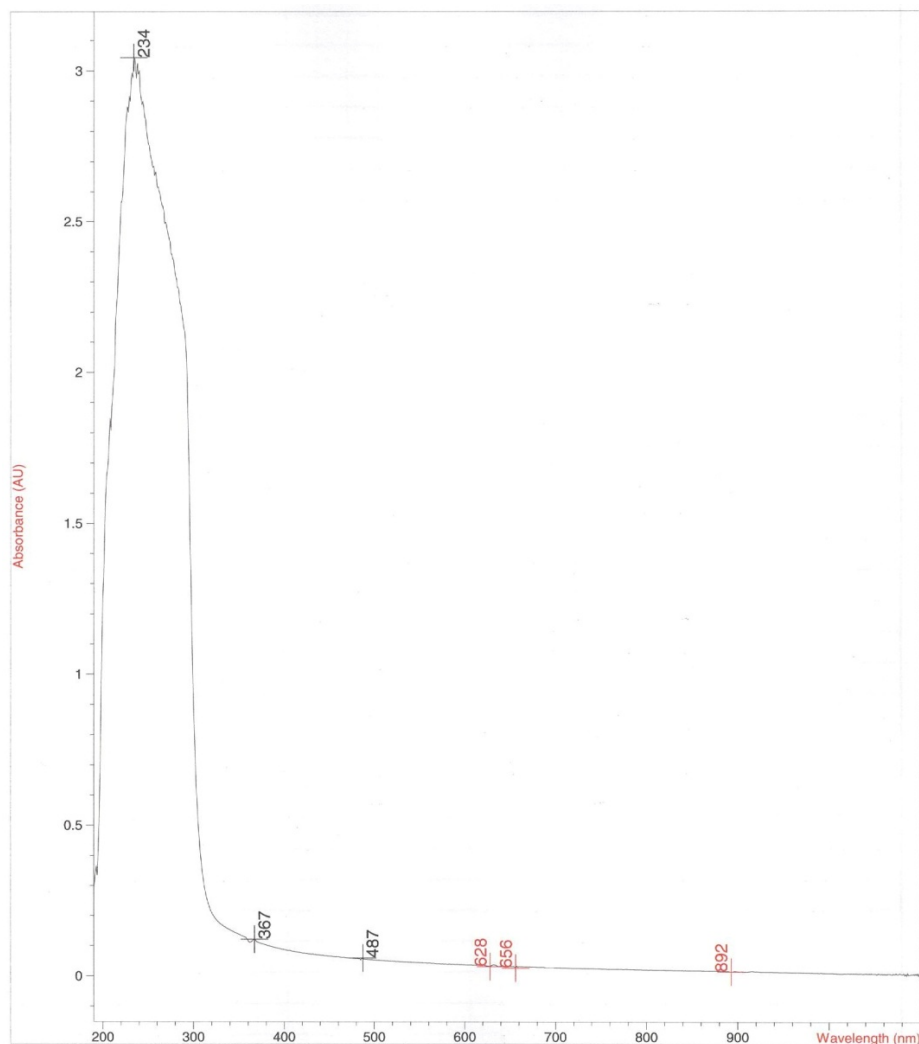


**Figure 17:** UV-Visible spectrum of MDTO in Hexane

### *Demonstration of Photoinduced Plasticity*

**Quantitative demonstration.** The stress relief experiments performed with the synthesized PETMP-TEGDVE MDTO copolymers was aimed at reproducing the demonstration carried out by Bowman et al.<sup>1</sup> **Figure 18** shows the plot of tensile stress measured as a function of time when the samples are stretched and irradiated at 366 nm wavelength.

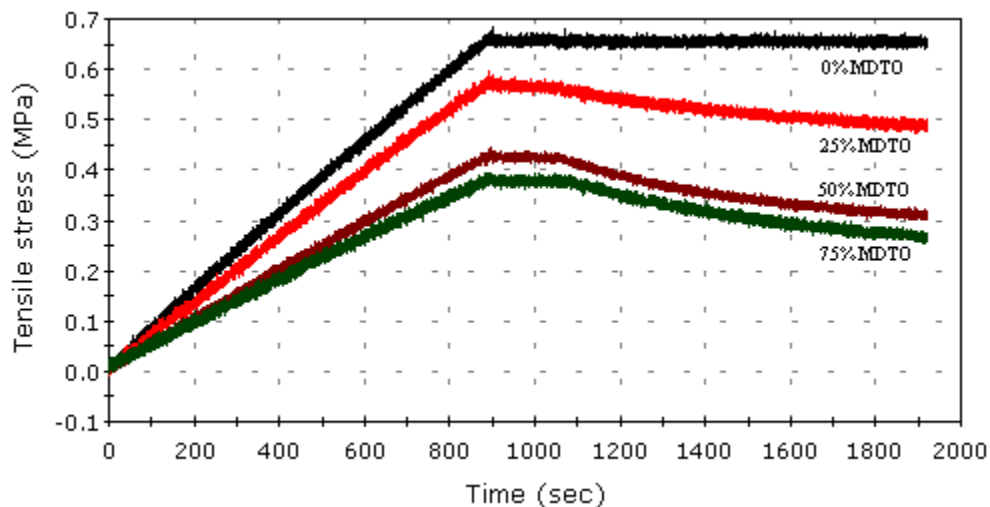


**Figure 18:** Stress relaxation plot at constant strain of 6%.

The first 900 seconds on the plot, where tensile stress increases with time, occurred when the samples were gradually stretched to the required level of strain (6%). Once the samples reached 6% strain, they were held at constant strain for 120 seconds, at which time irradiation was initiated. Upon irradiation, relaxation of stress was recorded as a gradual decrease in the tensile stress value with time. For the sample containing 0% MDTO, stress was relaxed upon irradiation. This was expected, given the fact that the requisite functionality for addition-fragmentation processes to occur is not present at 0% MDTO. As the concentration of MDTO increases, the concentration of photoactive allyl thioether groups in the network is greater and, thus, increased stress relief is observed.



**Qualitative demonstration.** The shape change occurring as a result of stress relief was demonstrated in this experiment. **Figure 19** shows the pictures of (a) stressed samples before irradiation and stress relief and (b) change of shape achieved post-irradiation.

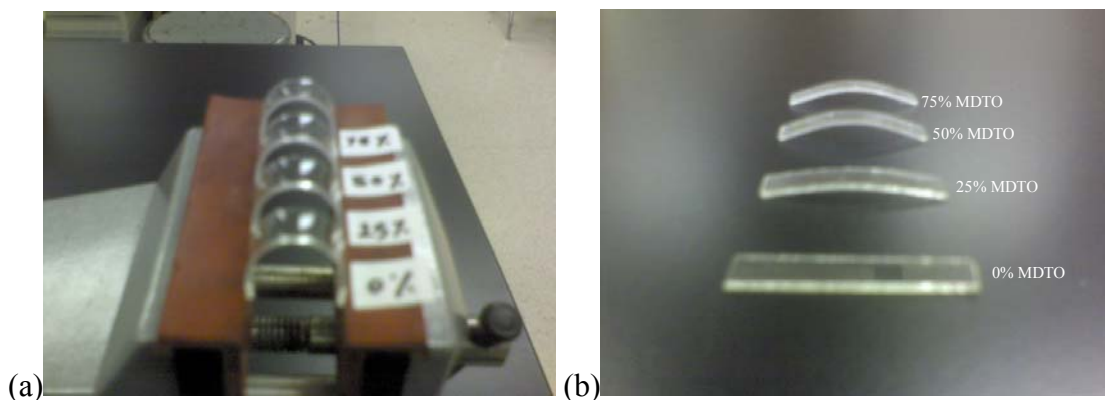


**Figure 19:** (a) stressed samples before irradiation (b) change of shape achieved after irradiation.

The initial shape of the samples in their non-stressed state was similar to that of the 0% MDTO sample in figure (b). The thicknesses of the samples were 1 mm and the concentration of the free radical initiator DMPA was 0.1%. At a wavelength of 366 nm, this DMPA level leads to optical opacity and a gradient in the absorption of light through the film thickness. The samples containing MDTO changed shape to a new state because of the photochemically induced gradient in stress relaxation across the film thickness. The magnitude of the change of shape that persists after irradiation on one side and release from torsion increased in proportion to the MDTO concentration. The film with no MDTO reverted back to its original shape after torsional stress was released.

### ***Photoplasticity in Siloxanes***

Photoinduced plasticity in crosslinked siloxane polymers is an extension of the chemistry demonstrated by Bowman et al. in traditional carbon chain polymers.<sup>1, 38</sup> Reproducing the results of Bowman et al. in our laboratory serves as a control in our observation of alternative thiol-ene polymer systems. In order to transition from the polymer systems used in the proof of

concept experiments to a new set of systems in the siloxane regime, it was necessary to start by creating a mimic of the traditional PETMP-TEGDVE-MDTO system.

The PETMP-TEGDVE-MDTO copolymer system was mimicked in siloxanes by applying the existing knowledge of thiol-ene siloxanes. PETMP, a tetra functional thiol was replaced by a commercially available multifunctional polydimethylsiloxane thiol, Gelest SMS-042, (THIOL.SIL) with a molar mass of 7600 g/mol and an average functionality of 4.82. TEGDVE was replaced by an end-functional vinyl siloxane, Gelest DMS-V21, with a molar mass of 6000 g/mol (VINYL.SIL). The photo-active co-monomer, MDTO, was kept constant. Prior to copolymerizing the siloxane thiol-ene mixture with MDTO, a neat thiol-ene mixture was copolymerized using DMPA as a photoinitiator. The result was a clear crosslinked siloxane polymer film.

**THIOL.SIL-VINYL.SIL-MDTO copolymer.** On attempting to copolymerize THIOL.SIL-VINYL.SIL with MDTO in bulk, it was observed that the monomer mixture was incompatible at room temperature and phase separated instantaneously. The mixture, however, became substantially clear when heated to a temperature of 65-70 °C or greater. Dicumyl peroxide, a high temperature free radical initiator was incorporated in the system in order to ensure that the half-life of the initiator at temperatures in excess of 70 °C was sufficient. On polymerization, the monomer mixture was observed to form a stable emulsion. In an effort to enhance compatibility, 25% by weight of toluene was incorporated in the same monomer system. Although the toluene-diluted monomer system was clear, when polymerization was initiated with AIBN at 70 °C, an emulsion was again obtained.

A noticeable characteristic of the emulsions formed is that they exhibit a bluish tinge associated with the Tyndall-effect of light scattered from submicron size particles in the

emulsion. The emulsion was dissolved in chloroform-d and NMR spectra were acquired. The instantaneous dissolution of the emulsion particles showed that the particles were not crosslinked gels. **Figure 20** shows the spectrum obtained for THIOL.SIL-VINYL.SIL-MDTO copolymer.

It can be clearly seen from the NMR data that the vinyl end groups in the emulsion remained largely unreacted. More importantly a pattern of peaks, a signature, characteristic of the homopolymer of MDTO can be seen. **Figure 20** shows  $^1\text{H}$ -NMR for the MDTO homopolymer obtained from literature<sup>66</sup> and **Figure 21** shows  $^1\text{H}$ -NMR for the THIOL.SIL-VINYL.SIL-MDTO copolymer, with peaks a-g being reflected in the  $^1\text{H}$ -NMR spectrum of the copolymer.

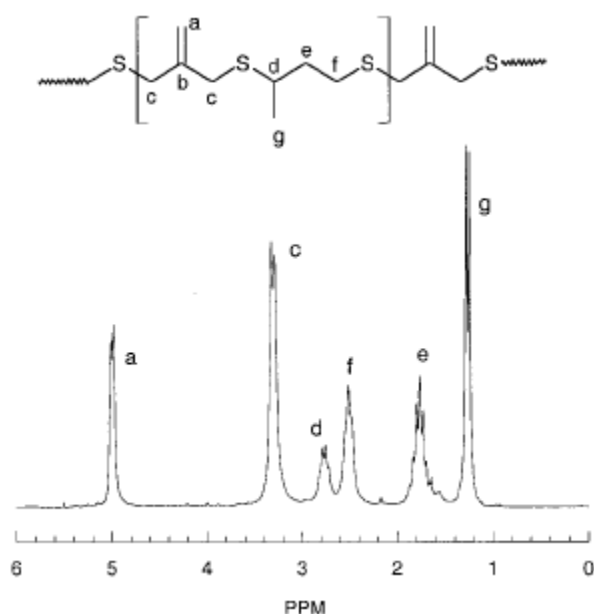


**Figure 20:**  $^1\text{H}$ -NMR of MDTO homopolymer (ref. 66)

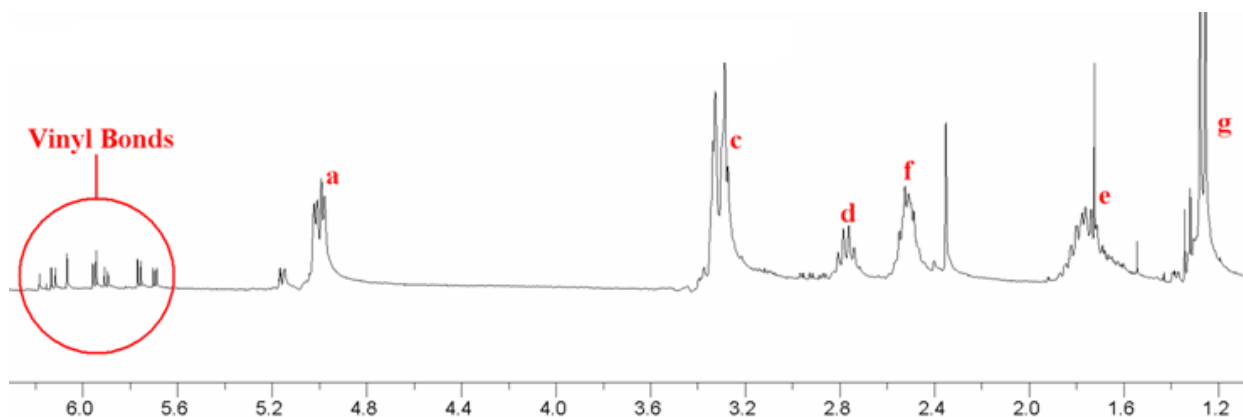


**Figure 21:**  $^1\text{H}$ -NMR for THIOL.SIL-VINYL.SIL-MDTO copolymer

**THIOL.SIL-NORB.SIL-MDTO copolymer.** In order to achieve a higher ene reactivity the vinyl end functional, VINYL.SIL was replaced with an end-functional norbornene siloxane, Gelest DMS-NB25, [NORB.SIL] having a molar mass of 14000 g/mol. The ring strain present in a norbornene makes the alkene double bond highly reactive and more susceptible to attack by a thiyl radical followed by ring opening. On solution polymerization of a THIOL.SIL-NORB.SIL-MDTO mixture in toluene using AIBN initiator at 70 °C, an emulsion similar in physical appearance to the one obtained using VINYL.SIL was obtained. The emulsion possessed a blue tinge characteristic of the presence of submicron sized particles.  $^1\text{H}$ -NMR of the emulsion was obtained in chloroform-d solvent and **Figure 22** shows the spectrum obtained.

It is clear from the  $^1\text{H}$ -NMR spectrum that the norbornene double bonds have substantially reacted to covalently incorporate NORB.SIL into a triblock polymer. The persistence of the MDTO homopolymer signature again confirms the presence of long, ring-opened MDTO homopolymer chain segments.

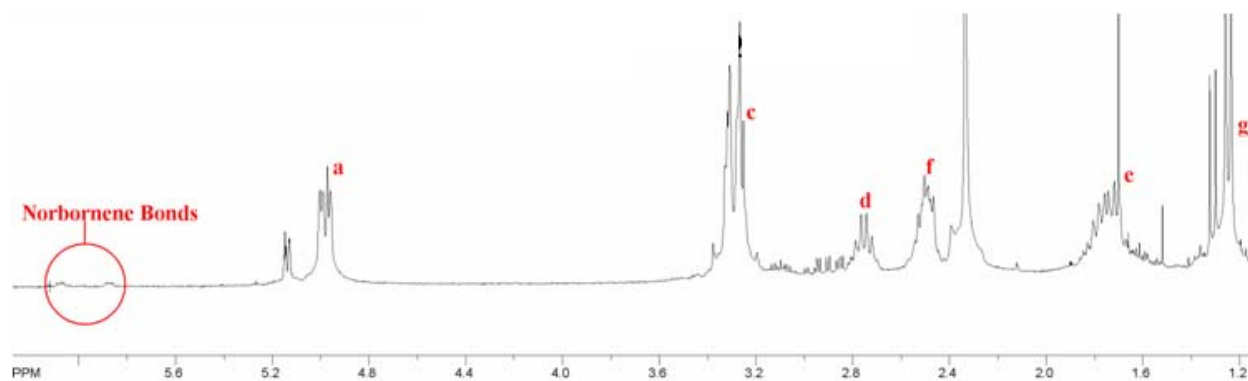


**Figure 22:**  $^1\text{H}$ -NMR of THIOL.SIL-NORB.SIL-MDTO copolymer

**THIOL.SIL-METHAC.SIL-MDTO copolymer.** In addition to reacting with thiol radicals,  $\alpha,\beta$ -unsaturated acrylics can add thiols by a Michael reaction using an end-functional methacrylate siloxane having a molar mass of 1830 g/mol [METHAC.SIL]. Solution polymerization of a composition comprising of a mixture of THIOL.SIL-METHAC.SIL-MDTO in toluene initiating with AIBN initiator at 70 °C, however, yielded an emulsion similar in appearance to the one obtained using VINYL.SIL. The emulsion exhibited a blue tinge characteristic of Tyndall scattering from submicron sized particles and the  $^1\text{H}$ -NMR obtained when the emulsion was dissolved in chloroform-d shows the MDTO homopolymer signature along with peaks indicative of the presence of a significant fraction of unreacted METHAC.SIL.

**Figure 23** shows the spectrum obtained.

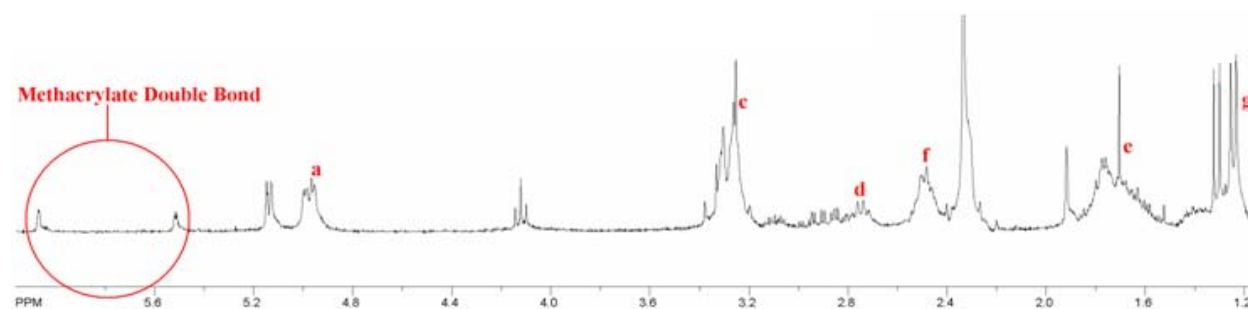


**Figure 23:**  $^1\text{H}$ -NMR of THIOL.SIL-METHAC.SIL-MDTO copolymer

**THIOL.SIL-TEGDVE-MDTO copolymer.** Vinyl ethers are perhaps the most reactive of all alkenes in the thiol-ene reaction and TEGDVE reacts with PETMP and MDTO to yield clear, homogeneous, gels. Accordingly, in an attempt to copolymerize THIOL.SIL with MDTO the polyether alkene, TEGDVE, was used as the ene component. Thus, a THIOL.SIL-TEGDVE-MDTO mixture, diluted with 25% by weight of toluene was copolymerized using AIBN initiator at 70 °C. The reaction again yielded an emulsion similar in appearance to the ones obtained using VINYL.SIL, NORB.SIL and METHAC.SIL. The  $^1\text{H}$ -NMR spectrum clearly shows that the vinyl ether bonds have reacted completely, however, the MDTO homopolymer signature persists indicating the presence of significant chain sequences containing ring-opened MDTO moieties. **Figure 24** shows the spectrum obtained.

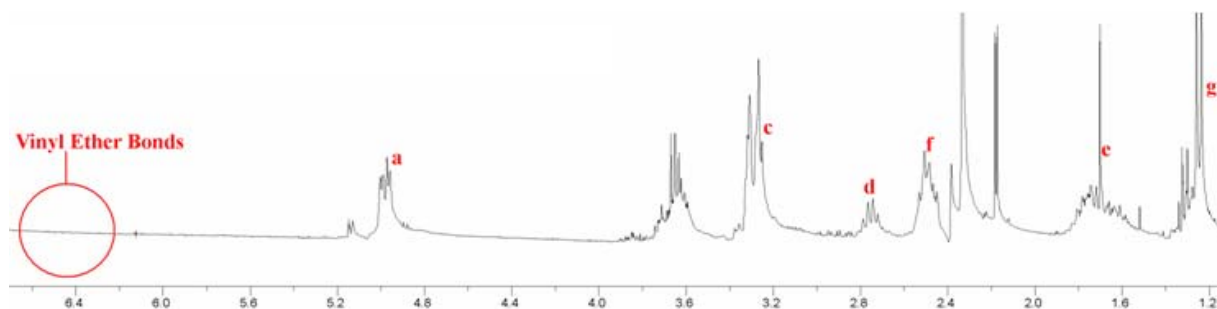


**Figure 24:**  $^1\text{H}$ -NMR spectrum for THIOL.SIL-TEGDVE-MDTO copolymer

The  $^1\text{H}$ -NMR data obtained from the copolymerizations carried out using THIOL.SIL with a variety of enes display two common features. First, all the emulsions exhibited a bluish tinge characteristic of Tyndall scattering from submicron sized particles. Second, the MDTO homopolymer signature was apparent in all the NMR spectra. The siloxane-based vinyl ene, VINYL.SIL, was substantially unreacted. The siloxane-based norbornene and methacrylate enes, NORB.SIL and METHAC.SIL, were more reactive, but peaks for unreacted alkene could still be seen in their  $^1\text{H}$ -NMR spectra. The alkenyl groups in the polyether-vinyl ether, TEGDVE, reacted completely. These data lead to the hypothesis that the copolymerization is initiated by

hydrogen abstraction from THIOL.SIL followed by the addition of a thiyl radical to MDTO and its ring-opening, chain-growth polymerization to generate long MDTO homopolymer chain segments. In the presence of TEGDVE and NORB.SIL, thiyl radicals on THIOL.SIL and ring-opened MDTO chains add. In the presence of VINYL.SIL and METHAC.SIL, alkenyl functionality remains substantially unreacted. The MDTO homopolymer chains apparently collapse and precipitate forming submicron-sized particles. The tethered siloxane chains form a corona that stabilize the particles against continued accretion, yielding a sterically stabilized emulsion of diblock or triblock copolymer particles. **Figure 25** shows a cartoon of the predicted particle structure.

**Figure 25:** Predicted particle structure for emulsions formed with THIOL.SIL

chain-extended Type 2 radical. When homopolymerization of MDTO is the dominant process in the reaction, the Type 2 radical shows a higher tendency towards route [B] compared to route [A].

The highlighted loop in the picture shows the initial formation of Type 1 radical followed by its attack on MDTO to create a Type 2 radical. The attack of this radical of MDTO following route [B] creates a diblock copolymer like structure. When all the MDTO monomers units in the reaction mixture are consumed in the process, the free radicals present at the chain ends then add to the ene at a rate dependent on the relative reactivity of the ene. In case the vinyl enes, the reaction to form triblock is limited. Vinyl ether bonds, on the other hand, being highly reactive readily forms the triblock and are consumed to the extent that no NMR signals for vinylic hydrogens can be observed post polymerization.

A similar process may be occurring in the Bowman type polymers used for the stress relaxation exercise. The only difference being that, irrespective of whether the Type 1 radical first attacks MDTO or the ene, the Type 2 radical always shows equal or nearly equal tendency to adopt either routes [A] and [B]. Thus, the allyl thioether groups present in the Bowman type system may be isolated monomeric units, or oligomeric block units which are distributed randomly in the crosslinked network. Higher concentration of MDTO would certainly tend to give slightly longer oligomeric blocks.



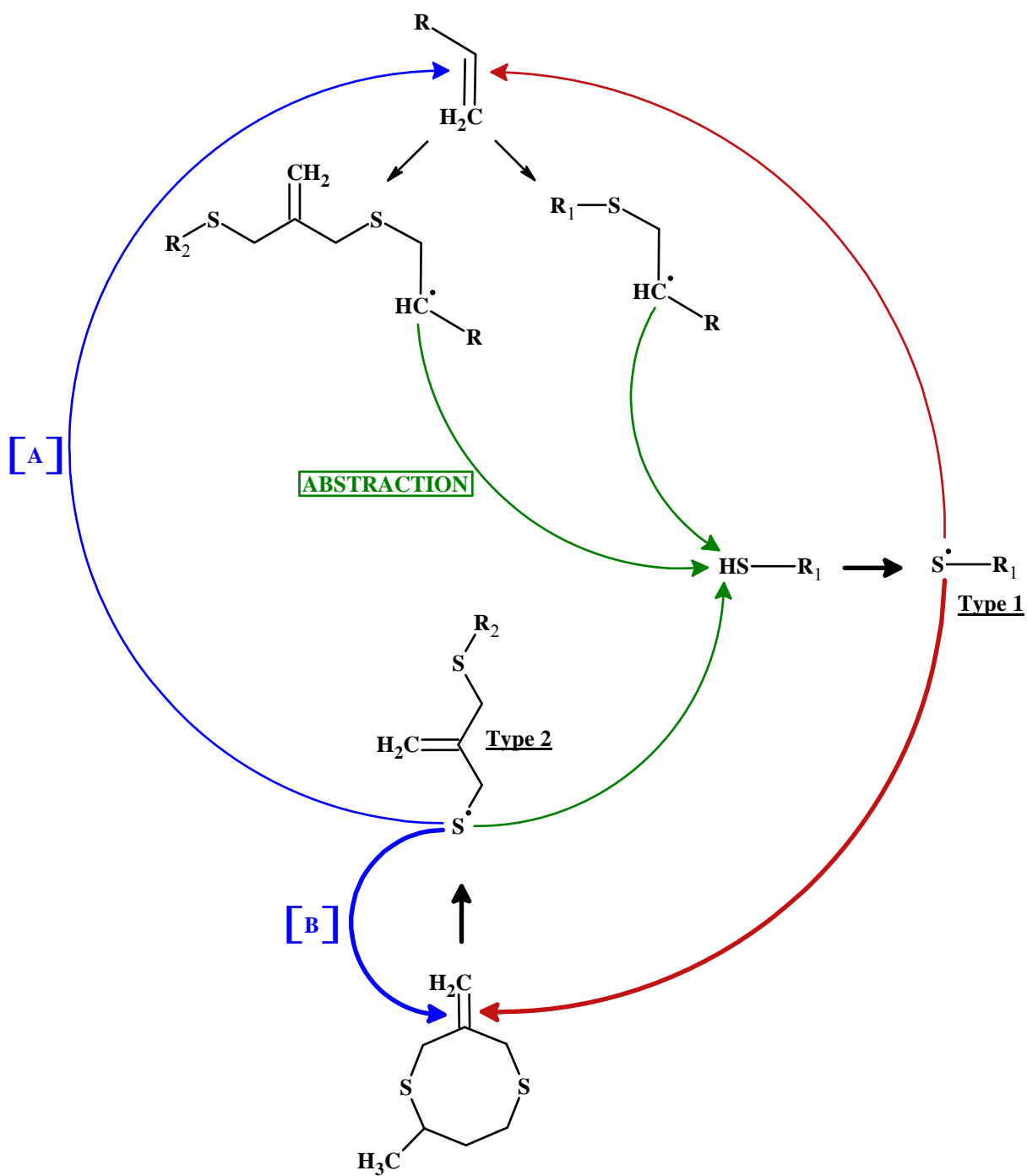


**Figure 26:** Free radical events occurring in a thiol-ene-MDTO copolymer system

### *Characterization of Emulsions*

**DLS data.** The emulsions obtained with THIOL.SIL were analyzed using DLS. The data shows a range of particle sizes for all emulsions synthesized. The number average size is about 3-4 times smaller than the intensity average size. This confirms the fact that the particle sizes are polydisperse.

Ene Component	Size by # Wt. (nm)	Size by Intensity Wt. (nm)
VINYL.SIL	29.2	108.4
NORB.SIL	48.4	187.6
METHAC.SIL	72.3	209
TEGDVE	20.1	90.2
VINYL.SIL (Photopolymerized)	89.8	249.8

**Table 3:** DLS data for emulsions obtained using THIOL.SIL

**TEM data.** The data obtained from DLS was corroborated with the TEM data and shows good correlation. **Figure 27** shows the images obtained for a THIOL.SIL-NORB.SIL-MDTO copolymer emulsion.

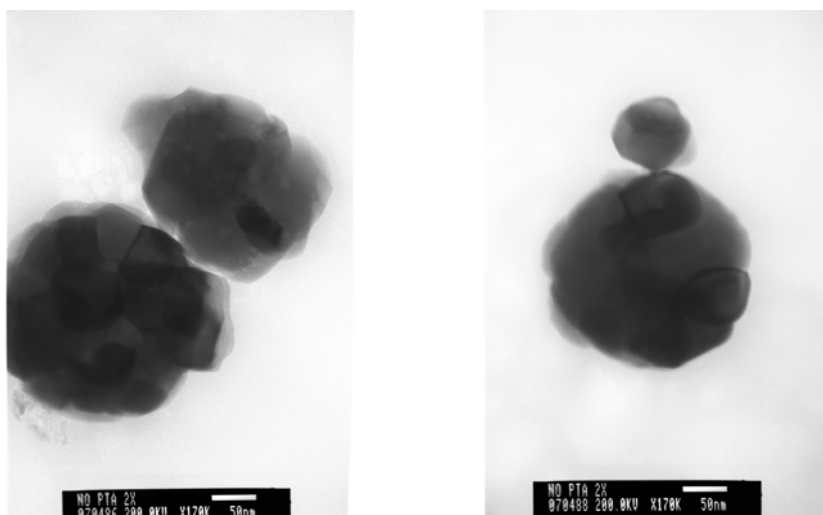


**Figure 27:** TEM images of THIOL.SIL-NORB-SIL-MDTO copolymer emulsion

The TEM images shown above are captured on a 50 nm scale. As seen, each large particle appears to be an aggregation of a number of smaller sub-particles. The sub-particle forms the primary structure and has a size of ~50 nm. The size of the larger aggregated particle may vary depending on the number of sub-particles aggregating together. The size of the aggregated particle shown in the picture above falls in the range of ~ 200 nm. These values are a good fit to the values obtained by DLS analyses. As seen in **Table 3**, the number average size for the NORB.SIL emulsion is 48.4 nm which correlates to the primary sub-particle size. The intensity average size obtained is 187.6 nm which is close to the aggregated particle size. TEM imaging of the emulsions obtained with VINYL.SIL, METHAC.SIL and TEGDVE was attempted, but clear images could not be obtained due to lack of good contrast.

Thus, the range of particle sizes observed [~ 50–200 nm] is supportive of the Tyndall blue effect observed in all the emulsions. The small particle sizes lead to scattering such that the emulsions appear to have a bluish tinge.

### ***Photoinitiated Polymerizations***

Photolytic radical generation process differs from thermal radical generation such that in a photolytic process a large number of radicals can be generated at the same instant. In a thermal process the rate of radical generation is distributed over a period of time, thus resulting in longer polymerization time periods. This ability to create a large number of radicals photochemically at any given instant is seen to have a significant effect on the crosslinking kinetics of the systems under investigation. Photoinitiated copolymerizations were carried out for systems containing THIOL.SIL copolymerized with MDTO and the full range of ene monomers at a wavelength of 366 nm. The observations and results noted are reported as follows.

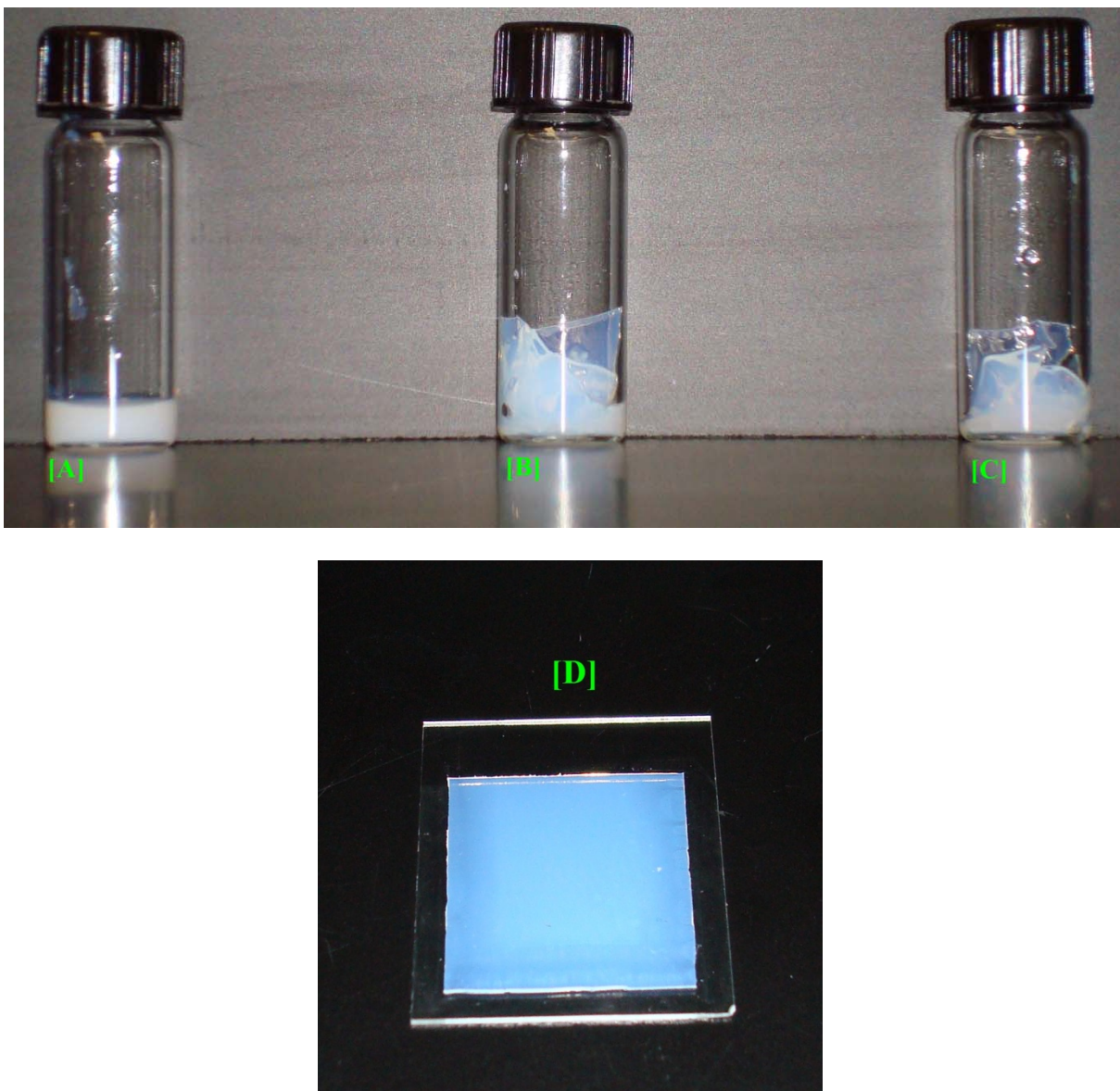
**Photo initiated THIOL.SIL-VINYL.SIL-MDTO copolymer.** Polymerization on a silanized glass plate yields an emulsion which possesses a bluish tinge associated with the Tyndall-effect of light scattered from submicron size particles. The emulsion obtained is much more viscous than its thermally polymerized counterpart and clearly has higher gel content. Although complete crosslinking did not take place since a swollen gel film could not be recovered from the glass place. **Figure 28(A)** shows a picture of the polymer after being transferred to a glass vial.

**Photo initiated THIOL.SIL-NORB.SIL-MDTO copolymer.** Polymerization with NORB.SIL on a silanized glass plate yields a partially crosslinked polymer which possesses a bluish tinge associated with the Tyndall-effect of light scattered from submicron size particles. Due to incomplete crosslinking the swollen gel could not be recovered from the glass plate without disintegration of the film. **Figure 28(B)** shows a picture of the polymer after being transferred to a glass vial.

**Photo initiated THIOL.SIL-METHAC.SIL-MDTO copolymer.** Like NORB.SIL, polymerization with METHAC.SIL on a silanized glass plate yields a partially crosslinked polymer which possesses a bluish tinge associated with the Tyndall-effect of light scattered from submicron size particles. Due to incomplete crosslinking, the swollen gel could not be recovered from the glass plate without disintegration of the film. **Figure 28(C)** shows a picture of the polymer after being transferred to a glass vial.

**Photo initiated THIOL.SIL-TEGDVE-MDTO copolymer.** Copolymerization with TEGDVE on a silanized glass plate yields a solvent swollen gel which possesses a bluish tinge associated with the Tyndall-effect of light scattered from submicron size particles. The mass may be completely crosslinked, since the solvent swollen film could be recovered from the glass plate

without disintegration. On drying the film to evaporate the solvent, a crosslinked siloxane film was obtained in which the blue tinge persisted. **Figure 28(D)** shows a picture of the gel polymer film after drying in the oven.



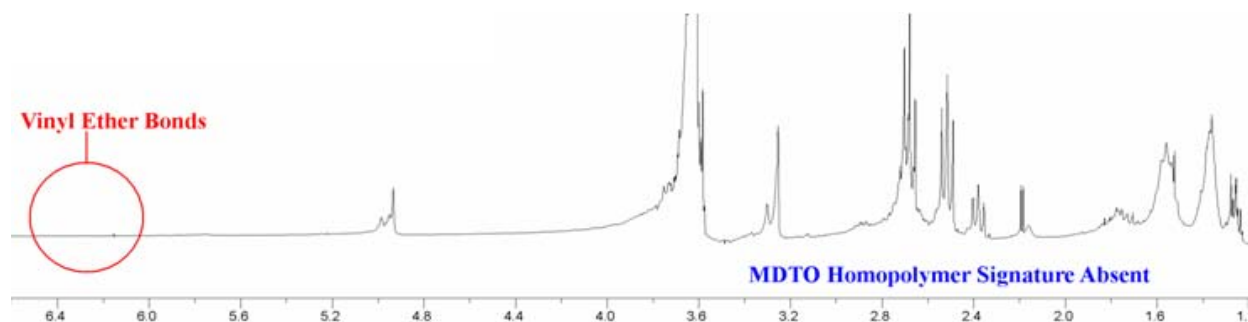
**Figure 28:** Photoinitiated copolymers of THIOL.SIL-MDTO with (A) VINYL.SIL. (B) NORB.SIL and (C) METHAC.SIL (D) TEGDVE

Photo initiation shows higher crosslinking tendencies compared to thermal initiation. The speculated cause for such behavior with photo initiators is related to the kinetic processes occurring during radical generation, and can be explained using the free radical events depicted in **Figure 26**. During photo initiation, at any given instant, there are a very large number of primary free radicals generated, as a result of which there is an excess of Type 1 radicals. The highlighted loop in the picture shows the initial formation of Type 1 radical followed by its attack on MDTO to create a Type 2 radical. Thus there is in turn an excess of Type 2 radicals present in the reaction mixture. Though the tendency of Type 2 radicals to adopt route [B] over route [A] persists, the number of those radicals present is large enough for a significant fraction to attack the ene following route [A]. The fact that route [B] is still favored over route [A] causes the formation of long MDTO homopolymer chains which eventually lead to submicron sized particles, rendering the Tyndall blue effect. Attack of the excess Type 2 radicals on the ene and the degree of crosslinking achieved depends on the activity of the ene. In case of VINYL.SIL, attack through route [A] is not as significant as it is in case of TEGDVE due to which the higher crosslinking is achieved with TEGDVE.

### ***Copolymers with HDT***

The tendency of MDTO to homopolymerize in a siloxane thiol-ene copolymer mixture was studied using  $^1\text{H}$ -NMR. We know that in Bowman type polymer systems, solution  $^1\text{H}$ -NMR cannot be obtained, because the polymers are solid gels. Thus, in order to investigate the polymerization characteristics of MDTO using solution NMR, a linear copolymer system analogous to Bowman type gels was created by replacing PETMP by HDT in the polymerization mixture.

**HDT-TEGDVE-MDTO copolymer.** Copolymerization of HDT with METHAC.SIL and MDTO in toluene using AIBN at a temperature of 70 °C yielded clear white viscous polymer. Formation of the emulsion did not occur. **Figure 29** shows  $^1\text{H}$ -NMR data obtained for the emulsion in chloroform-d solvent.



**Figure 29:**  $^1\text{H}$ -NMR for HDT-TEGDVE-MDTO copolymer

It is clear from the NMR spectrum that the vinyl ether double bonds react completely in the mixture. One can also see that the MDTO homopolymer signature does not exist. This means that the long homopolymer chains of MDTO are absent and allyl thioether functionality is incorporated randomly in the copolymer. This surrogate system to the Bowman type gels suggests that formation of emulsion occurs only when MDTO shows a tendency to homopolymerize. In other words, a clear transparent polymer can be formed only when the ring-opened MDTO units are incorporated randomly throughout the network.

The ene component in the linear, surrogate Bowman system polymerized was later replaced with the range of siloxane enes and the mixtures polymerized thermally. The observations recorded are given below.

**HDT-VINYL.SIL-MDTO copolymer.** Copolymerization of HDT with VINYL.SIL and MDTO in toluene using AIBN at a temperature of 70 °C yielded an emulsion which was milky white in appearance. The blue tinge obtained using THIOL.SIL was missing due to the absence

of small sub-micron sized particles. **Figure 30** shows  $^1\text{H}$ -NMR data obtained for the emulsion in chloroform-d solvent.

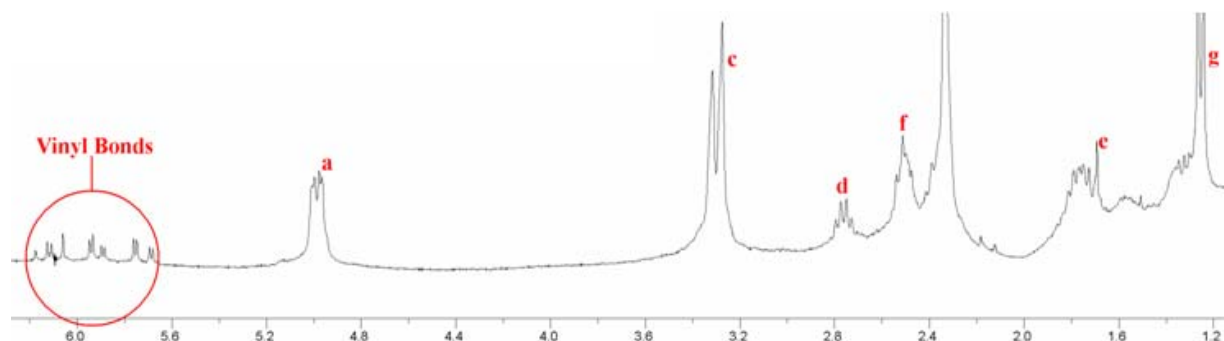


**Figure 30:**  $^1\text{H}$ -NMR for HDT-VINYLSIL-MDTO copolymer

NMR data shows that the vinyl double bonds remain unreacted in the reaction mixture. The MDTO homopolymer signature exists which means that the long MDTO homopolymer segments form a block copolymeric structure by reacting with the dithiol. This is unlike THIOL.SIL where the homopolymer chains are tethered at multiple locations to the siloxane chain leading to formation of extremely small micron sized particles as shown in **Figure 25**.

**HDT-NORB.SIL-MDTO copolymer.** Copolymerization of HDT with NORB.SIL and MDTO in toluene using AIBN at a temperature of 70 °C yielded an emulsion which was milky white in appearance. The blue tinge obtained using THIOL.SIL was missing when HDT was used since the small micron size particle formation did not take place. **Figure 31** shows  $^1\text{H}$ -NMR data obtained for the emulsion in chloroform-d solvent.

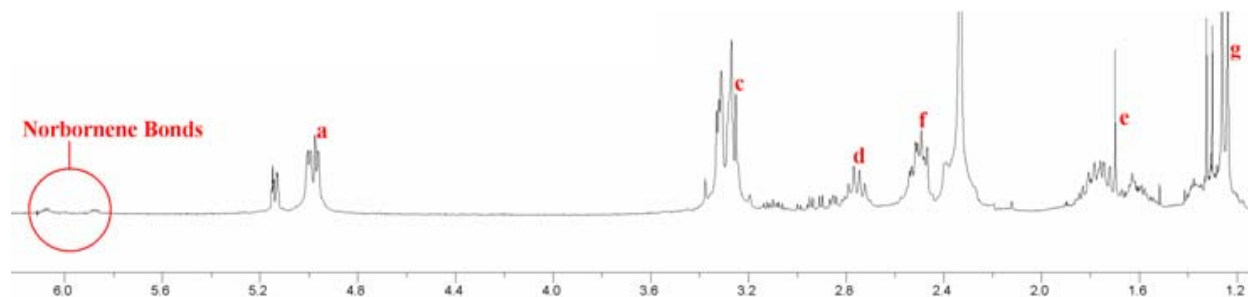


**Figure 31:**  $^1\text{H}$ -NMR for HDT-NORB.SIL-MDTO copolymer



NMR data shows that though the norbornene double bonds react in the mixture, some residual unsaturation still remains. The MDTO homopolymer signature exists which means that the long MDTO homopolymer segments for a block copolymeric structure by reacting with the dithiol. This is unlike THIOL.SIL where the homopolymer chains are tethered at multiple locations to the siloxane chain leading to formation of extremely small sub-micron sized particles.

**HDT-METHAC.SIL-MDTO copolymer.** Copolymerization of HDT with METHAC.SIL and MDTO in toluene using AIBN at a temperature of 70 °C yielded an emulsion which was milky white in appearance. The blue tinge obtained using THIOL.SIL was missing when HDT was used since the small micron size particle formation did not take place. **Figure 32** shows  $^1\text{H}$ -NMR data obtained for the emulsion in chloroform-d solvent.

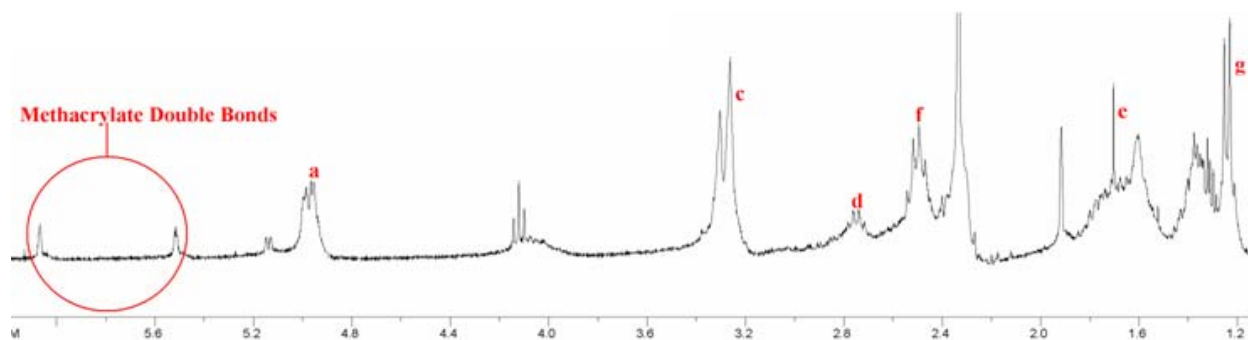


**Figure 32:**  $^1\text{H}$ -NMR for HDT-METHAC.SIL-MDTO copolymer

NMR data shows that though the methacrylate double bonds react in the mixture, some residual unsaturation still remains. The MDTO homopolymer signature exists which means that the long MDTO homopolymer segments for a block copolymeric structure by reacting with the dithiol. This is unlike THIOL.SIL where the homopolymer chains are tethered at multiple locations to the siloxane chain leading to formation of extremely small sub-micron sized particles.

The use of HDT as the thiol component yields linear polymers. As described in **Figure 26**, the first step occurring in the reaction mixture is the formation of Type 1 radical by hydrogen abstraction from a thiol group. Addition of this Type 1 radical to MDTO yields a Type 2 sulfide radical which prefers to follow route [B] over [A] to form long MDTO homopolymer chains. With HDT the homopolymer chains are present as linear block segments as compared to THIO.SIL where there is multiple number of MDTO homopolymer chains tethered to a single THIO.SIL chain. Thus, particles are formed in the HDT emulsions, which are not stabilized at a small enough size to render the Tyndall blue effect. Particles formed in the THIO.SIL emulsions are capable of reaching extremely small sub-micron particle sizes owing to the outer siloxane corona which provide steric stabilization, as shown in **Figure 25**.

#### ***Copolymers with PETMP***

The use of THIO.SIL with various functionalized siloxane enes for thiol-ene reactions with MDTO was described earlier in this thesis (pg. 31). Replacing THIO.SIL with HDT yields analogous linear polymer emulsions, just described. In an attempt to obtain a crosslinked system with an organic thiol, PETMP was substituted for HDT in combination with MDTO and various siloxane enes, specifically, VINYL.SIL, NORB.SIL and METHAC.SIL. While PETMP and the enes were miscible with each other in toluene, on mixing with PETMP the three-component mixture phase separated, instantaneously. As a result, polymerization could not be carried out. This marked incompatibility may be due to the fact that PETMP and HDT have substantially different solubility characteristics and solubility parameters; in PETMP, the thiol presents as a thiol-ester, whereas in HDT, the thiol presents as an alkyl thiol.

In the experimental work carried out so far with systems containing siloxane components, it appears that the propensity of the Type 2 thiyl radical to adopt route [B] over [A] is responsible

for MDTO homopolymerization. In thiol-ene systems containing MDTO and no siloxane monomers it appears that the propensity for Type 2 thiyl radical to adopt route [A] is comparable to its propensity to adopt route [B]. The HDT-TEGDVE-MDTO system yielding a clear linear polymer is an example of such a system. Accordingly, it can be stated that the presence of any siloxane, either the thiol, or the ene, or both, in copolymer systems containing MDTO results in the formation of grafted polymer emulsions have substantial MDTO homopolymer segments.

It might be argued that incipient immiscibility between siloxane oligomers and MDTO and/or MDTO chain segments during the polymerization induces the system to phase separate. Before polymerization begins, the co-solvent, toluene, keeps the system together and the solvated monomer mixture is clear. When the polymerization process begins and the first few units of MDTO are attached to the thiol, the mixture rapidly phase separates such that the radical chain end is confined in a micro or nano phase that is rich in MDTO. Such phase separation does not occur in the all-organic system and the any MDTO residues grafted to PETMP have equal access to ene molecules or MDTO. The radical chain in the all organic system will, thus, attack MDTO or the ene with nearly equal probability.

### **Conclusions and Future Directions**

Through the series of experiments reported in this thesis, an understanding of the copolymerization behavior of MDTO with thiol-enes was obtained. A hypothesis is offered to the effect that micro/nano phase separation occurs when MDTO is copolymerized with siloxane-based thiols and/or siloxane base –enes, and that this micro/nano phase separation results in homopolymerization and grafting of MDTO segments to initiating thiyl radicals. The essential incompatibility of the siloxane and MDTO graft-chain segments produces a sterically stabilized graft copolymer emulsion. The particle size and composition of these emulsions depends on the

type of ene used, nature of the thiol and type of initiation. Use of multi-functional thiol siloxanes yields emulsions with extremely small polydispersed particles ranging in size from 50 nm to 200 nm. The degree to which the ene component is covalently incorporated in the final composition depends on the reactivity of the ene component. Simple vinyl substituents bonded to Si are least reactive and are essentially not covalently incorporated into the graft copolymer. Methacrylate and norbornene double substituents are more reactive, however, their NMR spectra clearly show residual unsaturation.. Vinyl ether bonds are completely reacted.

Photoinitiation results in better incorporation of the ene component and the formation of crosslinked gel films. These gels films, however, are still heterogeneous and contain micro/nano domains of homopolymeric MDTO chain segments.

In order to obtain a clear crosslinked siloxane polymer containing allyl thioether functionality needed for photoplasticity, the allyl thioether moieties need to be randomly incorporated in the crosslinked network. Given the inherent incompatibility and phase separation issues associated with the use of MDTO as a comonomer with functional siloxanes, it is apparent that the allyl thioether groups need to be incorporated by a methodology other than the ring-opening of MDTO. A possible way to approach this problem might be to embed allyl thioether groups in a siloxane oligomer. MDTVE (shown in **Figure 10**) is a linear molecule bearing vinyl ether groups at the chain ends and an allyl sulfide group at the center. MDTVE has been reported to be synthesized by a process similar to that use to synthesize MDTO.<sup>38</sup>

Hydrosilylation one of the vinyl ether bonds in MDTVE by reacting with an oligomeric dimethylsiloxane-methylhydrosilane copolymer will allow allyl thioether groups to be incorporated pendant to the oligomeric siloxane backbone. Thus, by reacting the vinyl ether groups with a siloxane based thiol like THIOL.SIL, the issues relating to phase separation and

incompatibility might be circumvented. **Figure 33** shows a scheme for the proposed hydrosilylation reaction.

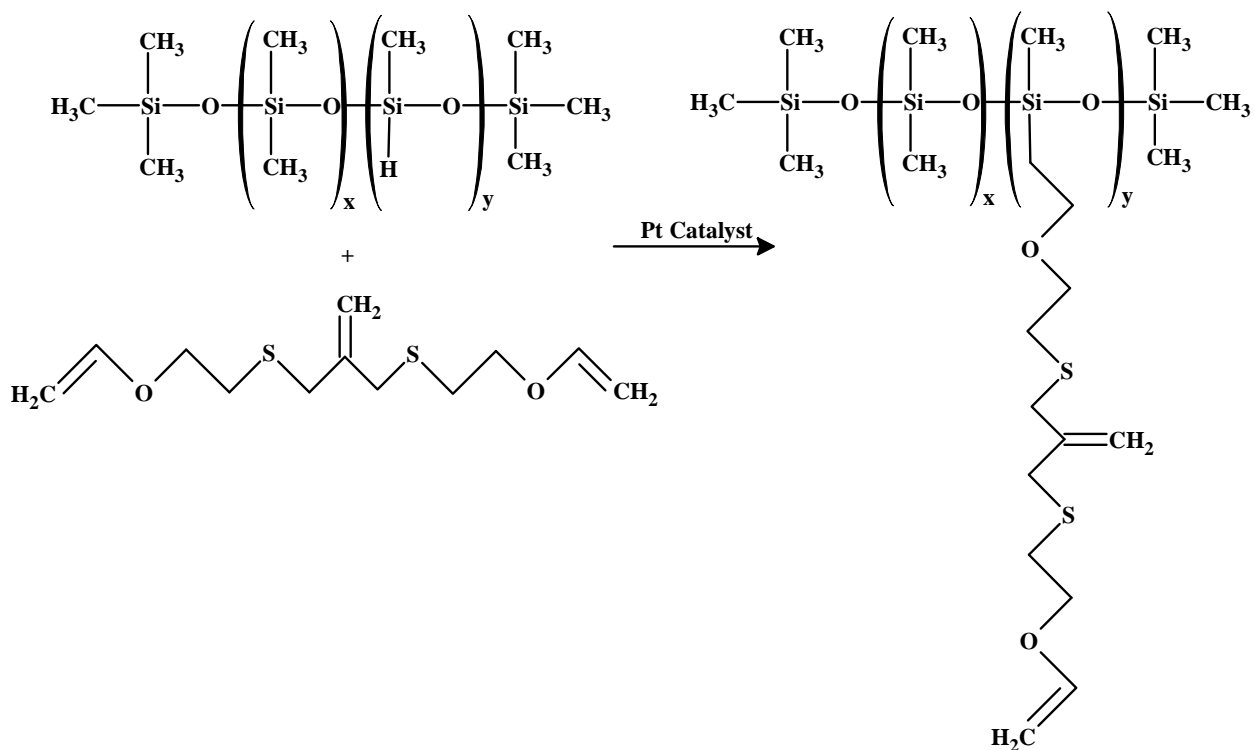


**Figure 33:** Proposed hydrosilylation of vinyl ether in MDTVE

Synthesis of clear crosslinked siloxane-based thiol-ene polymers would subsequently allow the demonstration of photoinduced plasticity in a manner similar to that demonstrated for the PETMP-TEGDVE-MDTO systems.

## References

1. Scott, T. F.; Schneider, A. D.; Cook, W. D.; Bowman, C. N., Photoinduced plasticity in cross-linked polymers. *Science* **2005**, 308, (5728), 1615-1617.
2. Behl, M.; Lendlein, A., Actively moving polymers. *Soft Matter* **2007**, 3, (1), 58-67.

3. Dietsch, B.; Tong, T., A review - Features and benefits of shape memory polymers (SMPs). *Journal of Advanced Materials* **2007**, 39, (2), 3-12.
4. Liu, C.; Qin, H.; Mather, P. T., Review of progress in shape-memory polymers. *Journal of Materials Chemistry* **2007**, 17, (16), 1543-1558.
5. Ratna, D.; Karger-Kocsis, J., Recent advances in shape memory polymers and composites: a review. *Journal of Materials Science* **2008**, 43, 254-269.
6. Behl, M.; Lendlein, A., Shape-memory polymers. *Materials Today* **2007**, 10, (4), 20-28.
7. Yu, Y. L.; Ikeda, T., Photodeformable polymers: A new kind of promising smart material for micro- and nano-applications. *Macromolecular Chemistry and Physics* **2005**, 206, (17), 1705-1708.
8. Jiang, H. Y.; Kelch, S.; Lendlein, A., Polymers move in response to light. *Advanced Materials* **2006**, 18, (11), 1471-1475.
9. Lendlein, A.; Jiang, H. Y.; Junger, O.; Langer, R., Light-induced shape-memory polymers. *Nature* **2005**, 434, (7035), 879-882.
10. Small, W.; Wilson, T. S.; Benett, W. J.; Loge, J. M.; Maitland, D. J., Laser-activated shape memory polymer intravascular thrombectomy device. *Optics Express* **2005**, 13, (20), 8204-8213.
11. Maitland, D. J.; Metzger, M. F.; Schumann, D.; Lee, A.; Wilson, T. S., Photothermal properties of shape memory polymer micro-actuators for treating stroke. *Lasers in Surgery and Medicine* **2002**, 30, (1), 1-11.
12. Cho, J. W.; Kim, J. W.; Jung, Y. C.; Goo, N. S., Electroactive shape-memory polyurethane composites incorporating carbon nanotubes. *Macromolecular Rapid Communications* **2005**, 26, (5), 412-416.
13. Mohr, R.; Kratz, K.; Weigel, T.; Lucka-Gabor, M.; Moneke, M.; Lendlein, A., initiation of shape-memory effect by inductive heating of magnetic nanoparticles in thermoplastic polymers. *Proceedings of the National Academy of Sciences* **2006**, 103, 3540-3545.
14. Ahir, S. V.; Tajbakhsh, A. R.; Terentjev, E. M., Self-assembled shape-memory fibers of triblock liquid-crystal polymers. *Advanced Functional Materials* **2006**, 16, (4), 556-560.
15. Finkelmann, H.; Benne, J.; Semmler, K., Smectic liquid single-crystal elastomers. *Macromolecular Symposia* **1995**, 96, 169-169.
16. Lehmann, W.; Skupin, H.; Tolksdorf, C.; Gebhard, E.; Zentel, R.; Kruger, P.; Losche, M.; Kremer, F., Giant lateral electrostriction in ferroelectric liquid-crystalline elastomers. *Nature* **2001**, 410, (6827), 447-450.
17. Hiraoka, K.; Finkelmann, H., Uniform alignment of chiral smectic C elastomers induced by mechanical shear field. *Macromolecular Rapid Communications* **2001**, 22, (6), 456-460.
18. Hiraoka, K.; Sagano, W.; Nose, T.; Finkelmann, H., Biaxial shape memory effect exhibited by monodomain chiral smectic C elastomers. *Macromolecules* **2005**, 38, (17), 7352-7357.

19. Tajbakhsh, A. R.; Terentjev, E. M., Spontaneous thermal expansion of nematic elastomers. *European Physical Journal E* **2001**, 6, (2), 181-188.
20. Terentjev, E. M.; Warner, M., Continuum theory of ferroelectric smectic C-asterisk elastomers. *Journal De Physique II* **1994**, 4, (5), 849-864.
21. Yang, Z. Q.; Huck, W. T. S.; Clarke, S. M.; Tajbakhsh, A. R.; Terentjev, E. M., Shape-memory nanoparticles from inherently non-spherical polymer colloids. *Nature Materials* **2005**, 4, (6), 486-490.
22. Benne, I.; Semmler, K.; Finkelmann, H., 2nd-Harmonic generation on mechanically oriented S(C)asterisk-elastomers. *Macromolecular Rapid Communications* **1994**, 15, (4), 295-302.
23. Benne, I.; Semmler, K.; Finkelmann, H., Mechanically induced 2nd-harmonic generation in S-C-asterisk elastomers. *Macromolecules* **1995**, 28, (6), 1854-1858.
24. Semmler, K.; Finkelmann, H., Mechanical field orientation of chiral smectic-C polymer networks *Macromolecular Chemistry and Physics* **1995**, 196, (10), 3197-3208.
25. Degennes, P. G., One type of nematic polymers. *Comptes Rendus Hebdomadaires Des Seances De L Academie Des Sciences Serie B* **1975**, 281, (5-8), 101-103.
26. Ichimura, K., Photoalignment of liquid-crystal systems. *Chemical Reviews* **2000**, 100, (5), 1847-1873.
27. Natansohn, A.; Rochon, P., Photoinduced motions in azo-containing polymers. *Chemical Reviews* **2002**, 102, (11), 4139-4175.
28. Tamai, N.; Miyasaka, H., Ultrafast dynamics of photochromic systems. *Chemical Reviews* **2000**, 100, (5), 1875-1890.
29. Irie, M., Photoresponsive polymers. *Advances in Polymer Science* **1990**, 94, 27-67.
30. Shibaev, V.; Bobrovsky, A.; Boiko, N., Photoactive liquid crystalline polymer systems with light-controllable structure and optical properties. *Progress in Polymer Science* **2003**, 28, (5), 729-836.
31. Meijs, G. F.; Rizzardo, E.; Thang, S. H., Preparation of controlled molecular-weight, olefin-terminated polymers by free-radical methods - Chain transfer using allyl sulfides. *Macromolecules* **1988**, 21, (10), 3122-3124.
32. Meijs, G. F.; Morton, T. C.; Rizzardo, E.; Thang, S. H., Use of substituted allylic sulfides to prepare end-functional polymers of controlled molecular weight by free-radical polymerization. *Macromolecules* **1991**, 24, (12), 3689-3695.
33. Sunder, A.; Mulhaupt, R., Addition-fragmentation free radical polymerization in the presence of olefinic dithioethers as chain transfer agents. *Macromolecular Chemistry and Physics* **1999**, 200, (1), 58-64.
34. Hoyle, C. E.; Lee, T. Y.; Roper, T., Thiol-enes: Chemistry of the past with promise for the future. *Journal of Polymer Science Part a-Polymer Chemistry* **2004**, 42, (21), 5301-5338.
35. Evans, R. A.; Moad, G.; Rizzardo, E.; Thang, S. H., New free-radical ring-opening acrylate monomers. *Macromolecules* **1994**, 27, (26), 7935-7937.
36. Evans, R. A.; Rizzardo, E., Free-radical ring-opening polymerization of cyclic allylic sulfides. *Macromolecules* **1996**, 29, (22), 6983-6989.

37. Evans, R. A.; Rizzardo, E., Free-radical ring-opening polymerization of cyclic allylic sulfides. 2. Effect of substituents on seven- and eight-membered ring low shrink monomers. *Macromolecules* **2000**, 33, (18), 6722-6731.
38. Scott, T. F.; Draughon, R. B.; Bowman, C. N., Actuation in crosslinked polymers via photoinduced stress relaxation. *Advanced Materials* **2006**, 18, (16), 2128-+.
39. Kharasch, M. S.; Read, A. T.; Mayo, F. R., Peroxide effect in the addition of reagents to unsaturated compounds. XVI. Styrene and isobutylene. *Chemistry & Industry* **1938**, 57, 752.
40. Marvel, C. S.; Chambers, R. R., Polyalkylene sulfides from diolefins and dimercaptans. *Journal of the American Chemical Society* **1948**, 73, 993-998.
41. Marvel, C. S.; Caesar, P. D., Polyalkylene sulfides. IX. Polyarylene-alkylene sulfides. *Journal of the American Chemical Society* **1951**, 73, 1097-99.
42. Bush, R. W.; Ketley, A. D.; Morgan, C. R.; Whitt, D. G., Comparative rate studies of uv-curable systems using a photocalorimetric device. *Journal of Radiation Curing* **1980**, 7, (2), 20-5.
43. Morgan, C. R. Urethane-thioether-containing polyene composition and reaction product. US 3784524, 1974.
44. Morgan, C. R.; Magnotta, F.; Ketley, A. D., thiol-ene photo-curable polymers. *Journal of Polymer Science Part a-Polymer Chemistry* **1977**, 15, (3), 627-645.
45. Morgan, C. R.; Ketley, A. D., Effect of phosphines on thiol-ene curing systems. *Journal of Polymer Science Part C-Polymer Letters* **1978**, 16, (2), 75-79.
46. Morgan, C. R.; Ketley, A. D., The photopolymerization of allylic and acrylic monomers in the presence of polyfunctional thiols. *Journal of Radiation Curing* **1980**, 7, (2), 10-13.
47. Patai, S., *Chemistry of Thiol Group*. Wiley: New York, 1974.
48. Jacobine, A. F., *Thiol-Ene Photopolymers*. Elsevier: London, 1993; Vol. 7.
49. Cramer, N. B.; Reddy, S. K.; O'Brien, A. K.; Bowman, C. N., Thiol-ene photopolymerization mechanism and rate limiting step changes for various vinyl functional group chemistries. *Macromolecules* **2003**, 36, (21), 7964-7969.
50. Roper, T. M.; Hoyle, C. E.; Guymon, C. A., Effect of double bond position on the reactivity of alkenes with a monofunctional thiol and its applications to thiol-ene crosslinking reactions. *Abstracts of Papers of the American Chemical Society* **2003**, 225, U543-U543.
51. Roper, T. M.; Guymon, C. A.; Jonsson, E. S.; Hoyle, C. E., Influence of the alkene structure on the mechanism and kinetics of thiol-alkene photopolymerizations with real-time infrared spectroscopy. *Journal of Polymer Science Part a-Polymer Chemistry* **2004**, 42, (24), 6283-6298.
52. Oswald, A. A.; Naegele, W., Organic sulfur compounds .19. Addition of dithiols to diallyl maleate - A new concept of polyester synthesis. *Makromolekulare Chemie* **1966**, 97, (SEP), 258-&.
53. Bexell, U.; Olsson, M.; Johansson, M.; Samuelsson, J.; Sundell, P. E., A tribological study of a novel pre-treatment with linseed oil bonded to mercaptosilane treated aluminium. *Surface & Coatings Technology* **2003**, 166, (2-3), 141-152.



54. Johansson, M.; Samuelsson, J.; Sundell, P. E.; Bexell, U.; Olsson, M., Radiation induced polymerization of monomers from renewable resources. *Abstracts of Papers of the American Chemical Society* **2003**, 225, U536-U536.
55. Woods, J. G.; Rakas, M. A.; Jacobine, A. F.; Alberino, L. M.; Kropp, P. L.; Sutkaitis, D. M.; Glaser, D. M.; Nakos, S. T. Optical fiber primary coating compositions. US 5459175, 1995.
56. Sangermano, M.; Bongiovanni, R.; Malucelli, G.; Priola, A.; Harden, A.; Rehnberg, N., Synthesis of new fluorinated allyl ethers for the surface modification of thiol-ene ultraviolet-curable formulations. *Journal of Polymer Science Part a-Polymer Chemistry* **2002**, 40, (15), 2583-2590.
57. Wan, Q. C.; Schrick, S. R.; Culbertson, B. M., Methacryloyl derivitized hyperbranched polyester. 1. Synthesis, characterization, and copolymerization. *Journal of Macromolecular Science-Pure and Applied Chemistry* **2000**, 37, (11), 1301-1315.
58. Wan, Q. C.; Schrick, S. R.; Culbertson, B. M., Methacryloyl derivitized hyperbranched polyester. 2. Photo-polymerization and properties for dental resin systems. *Journal of Macromolecular Science-Pure and Applied Chemistry* **2000**, 37, (11), 1317-1331.
59. Jacobine, A. F.; Glaser, D. M.; Grabek, P. J.; Mancini, D.; Masterson, M.; Nakos, S. T.; Rakas, M. A.; Woods, J. G., Photocrosslinked norbornene thiol copolymers - synthesis, mechanical properties, and cure studies. *Journal of Applied Polymer Science* **1992**, 45, (3), 471-485.
60. Gush, D. P.; Ketley, A. D., Thiol/acrylate hybrid systems. *Modern Paint and Coatings* **1978**, 68, (11), 58, 61-2, 64, 66.
61. Trieschmann, C.; Hockemeyer, F.; Preiner, G. Photocrosslinkable siloxane release coatings for paper.
62. LeGrow, G. E. 1972.
63. Jacobine, A. F.; Nakos, S. T., In *Radiation Curing: Science and Technology*, Pappas, S. P., Ed. Plenum: New York, 1992; p 181.
64. Muller, U.; Kunze, A.; Herzig, C.; Weis, J., Photocrosslinking of silicones .13. Photoinduced thiol-ene crosslinking of modified. *Journal of Macromolecular Science-Pure and Applied Chemistry* **1996**, A33, (4), 439-457.
65. Jacobine, A. F.; Glaser, D. M.; Nakos, S. T., In *Radiation Curing of Polymeric Materials*, Kinstle, J. F.; Hoyle, C. E., Eds. American Chemical Society: Washington DC, 1990; p 160.
66. Evans, R. A.; Rizzardo, E., Free radical ring-opening polymerization of cyclic allylic sulfides: Liquid monomers with low polymerization volume shrinkage. *Journal of Polymer Science Part a-Polymer Chemistry* **2001**, 39, (1), 202-215.